Energy Conversion and Management 179 (2019) 249–269

Contents lists available at ScienceDirect

Energy Conversion and Management

journal homepage: www.elsevier.com/locate/enconman

Exergy cost assessment of CSP driven multi-generation schemes: Integrating seawater desalination, refrigeration, and process heat plants

Roberto Leiva-Illanes[a,b,*], Rodrigo Escobar[c], José M. Cardemil[d], Diego-César Alarcón-Padilla[e], Javier Uche[f], Amaya Martínez[f]

[a] Escuela de Ingeniería, Pontificia Universidad Católica de Chile, Santiago, Chile
[b] Departamento de Mecánica, Universidad Técnica Federico Santa María, Viña del Mar, Chile
[c] Centro del Desierto de Atacama, Centro de Energía, Escuela de Ingeniería, Pontificia Universidad Católica de Chile, Santiago, Chile
[d] Departamento de Ingeniería Mecánica, Universidad de Chile, Santiago, Chile
[e] CIEMAT-Plataforma Solar de Almería, Almería, Spain
[f] Departamento de Ingeniería Mecánica, Instituto CIRCE, Universidad de Zaragoza, Zaragoza, Spain

ARTICLE INFO

Keywords:
Multi-generation
Symbolic thermoeconomic
Concentrated solar power
Multi-effect distillation
Refrigeration
Process heat

ABSTRACT

An exergy cost assessment of integrated solar multi-generation schemes, which includes cogeneration, trigeneration, and polygeneration schemes, for the joint production of electricity, fresh water, cooling, and process heat, is carried out. This evaluation process allows finding out the key equipment to improve the design, detect potential energy savings, and establish the best configurations of these schemes, in terms of unit exergy cost, total exergy cost, and exergy efficiency. The methodology includes modelling and evaluating the performance of solar multi-generation schemes and stand-alone systems, by applying the symbolic exergoeconomic methodology. The solar multi-generation schemes consider a concentrated solar power as the prime mover, which is coupled to a multi-effect distillation, an absorption refrigeration, and a process heat plant. Twenty-one configurations were investigated, twenty of them regarding solar multi-generation plants: eight of cogeneration, eight of trigeneration, four polygeneration schemes, and the other one considering stand-alone systems. This study reveals that the recommended configurations for the solar multigeneration schemes are those in which the desalination plant replaces the condenser of the power cycle, and the refrigeration plant, as well as the process heat module are coupled to turbine extractions. Furthermore, the main components contributing to the cost formation of electricity are, in this order, solar collectors, evaporator, and reheater. In the case of by-products generated, the main components are dissipative systems, solar collectors, and productive subsystems (multi-effect distillation, refrigeration, and process heat plants). In consequence, they constitute the key equipment that could be improved. Finally, solar multi-generation schemes are more cost effective than stand-alone systems. For instance, the best option within the polygeneration schemes analyzed allowed reducing the unit exergy cost about 6.8%, 59.2%, 45.6%, and 32.2% for electricity, water, cooling, and process heat respectively. Therefore, solar multi-generation schemes are identified as a promising alternative for zones with high irradiation conditions and scarcity of water, where the CSP technology can be the prime mover.

1. Introduction

Both multi-generation and polygeneration are the integration of multiple utility outputs, from one or more inputs, for improving the overall performance of energy systems. For the purpose of the analysis developed herein, when a multi-generation scheme generates two, three, or more products, it will be called a cogeneration, trigeneration, and polygeneration scheme, respectively. The performance of a multi-generation system may be assessed from different aspects, such as, thermodynamic, economic, environmental, and social issues. Thus, the main advantages delivered by those systems are measured in terms of the improvement of energy efficiency and cost-effectiveness, use of alternative fuels or energy carriers, and reduction of greenhouse gas emissions, among other indexes. Those advantages constitute multi-generation systems as a competitive technology compared to stand-alone plants delivering equivalent utilities [1]. In the topping cycle of a

* Corresponding author at: Departamento de Mecánica, Universidad Técnica Federico Santa María, Av. Federico Santa María 6090, Viña del Mar, Chile, and Escuela de Ingeniería, Pontificia Universidad Católica de Chile, Vicuña Mackenna 4860, Santiago, Chile.
E-mail addresses: roberto.leiva@usm.cl, rleivaillanes@puc.cl (R. Leiva-Illanes).

https://doi.org/10.1016/j.enconman.2018.10.050
Received 4 June 2018; Received in revised form 18 September 2018; Accepted 16 October 2018
Available online 27 October 2018

Nomenclature

A	solar field aperture area, m^2
BS	backup system
C	exergy cost, kW
$\mathbf{C}_P$	exergy cost of the product, kW
$\mathbf{C}_P^e$	exergy cost of product due to irreversibilities of the components, kW
$\mathbf{C}_P^r$	exergy cost of product due to the residues allocation, kW
c	unit exergy cost, kW/kW
$\mathbf{c}_e$	unit exergy cost of the external resources, kW/kW
$\mathbf{c}_R$	unit exergy cost of the residues, kW/kW
COP	coefficient of performance, -
CSP	concentrated solar power
CST	cold storage tank
E	exergy flow, kW
ECT	exergy cost theory
FWP	feed water preheater
F	fuel, kW
$\mathbf{F}_e$	vector of external resources
$\langle \mathbf{FP} \rangle$	matrix composed of distribution coefficients
G	generator
G_b	direct normal irradiance, W/m^2
HP	high pressure
HST	hot storage tank
I	irreversibility, kW
$\mathbf{K}_D$	diagonal matrix of unit exergy consumptions
k	unit exergy consumptions, kW/kW
LP	low pressure
MED	multi-effect distillation
P	product, kW
PH	process heat plant
Poly	Polygeneration
REF	Refrigeration plant
SF	solar field
TES	thermal energy storage
$\mathbf{U}_D$	identity matrix
V_D	dissipative system components
y	distribution coefficients

Greek symbols

ψ	exergy efficiency
β_{ir}	residue cost distribution ratio

multi-generation system [2], fuel is used in the prime mover, typically driving a power cycle such as Rankine, Brayton or Diesel, that generates electricity. Prime mover's hot exhaust is used to supply thermal energy to a secondary unit driven by heat, like thermal distillation, process heat, and/or absorption cooling. Using a Concentrated Solar Power (CSP) plant as a prime mover is an interesting alternative to analyze when it is implemented in a multi-generation scheme; since it produces electricity driven by solar energy and could be coupled to a thermal energy storage or be hybridized with fossil fuels or other renewable sources. That integration allows continuous operation, as well as developing capacity factors similar to those achieved by conventional power plants, enabling plant's dispatchability management, and additionally, taking advantage of the heat rejected from the power block. This heat could be recovered by thermally driven technologies, such as fresh-water, cooling, and process heat [3]. Regarding the thermal desalination technologies, the main technologies are multi-effect distillation (MED) and multi-stage flash (MSF), whereas the first is considered the most attractive option because it has low energy consumption, low sensitivity to corrosion, low presence of scaling, high development potential, and low operating temperature [4,5]. While that reverse osmosis (RO) represents the most reliable and commercially proven technologies for desalination, but it is driven by electricity, not allowing the use of the residual heat. About the refrigeration systems driven by thermal energy, single-effect absorption cycles are more appropriate since their operating temperatures are lower and present high market availability [4,5].

The integration of a CSP plant into a multi-generation scheme is a complex process that requires the use of robust methods in its assessment and optimization. In this context, there are several methods for evaluating the integration strategies in multi-generation schemes [1,6,7]. Among those methods the Thermoeconomic (or Exergoeconomic) method [8] is recommended because it provides a compact matrix formulation for the detailed analysis of complex systems based on the physical roots established by the Second Law of Thermodynamics [9]. Second Law establishes that in some energy carriers, part of the energy cannot be converted into useful energy. It assesses both quantity and quality of energy through a specific property called exergy, indicating the maximum amount of work that a flow or a system might produce while interacting with the environment. This method is very useful to analyze complex systems because it allows measuring, in the same physical unit, resources and waste flows of different nature, for instance electricity, fresh water, cooling or heat. Commonly, the rationale use of resources in complex systems is evaluated in terms of the exergy cost of mass and/or energy flows, which represents the units of consumed exergy to produce it, i.e. the exergy cost of a flow is the amount of resources expressed in exergy consumed for producing that flow [10]. The exergy cost allows analyzing and identifying integration possibilities because it enables determining the potential for resource savings. Exergy cost is a conservative magnitude that increases in every process according to the irreversibilities involved in it. In an integrated process, it is interesting to study in depth how exergy costs are formed, since the process of cost formation provides meaningful information that allows implementing significant improvements on the design and an accurate performance analysis. Moreover, this technique could assess the impact of a partial failure in any device of the multi-generation plant over the products costs and the primary energy consumption, what is known as the thermoeconomic diagnosis of the plant operation.

As described by Modi et al. [3] and Jana et al. [11], CSP technologies could be integrated into multi-generation schemes, with improvements in economics, environmental, and conversion efficiency terms. They presented comprehensive reviews of solar energy-based heat and power plants, and multi-generation schemes as a future sustainable energy solution, in which different studies have focused mainly on determining the final cost of each product by thermoeconomic methods. They concluded that multi-generation schemes constitute an efficient, environment friendly and a rational approach for exploiting the available natural resources. Currently, there is only one CSP plant configured in a cogeneration system, the "Aalborg CSP-Brønderslev CSP with Organic Rankine Cycle (ORC) project" located in Denmark, which comprises a 16.6 MW_{th} CSP plant for combined heat and power generation [4,5,12]. Regarding the thermoeconomic method, Al-Sulaiman et al. [13,14] carried out a thermoeconomic optimization of a CSP-trigeneration system, considering an organic Rankine cycle as the prime mover, an absorption chiller, and a process heat module. The specific exergy costing method was applied to conduct an evaluation of costs associated to each exergy stream entering and exiting system's components, aiming to determine the final cost (unit exergy cost and exergy cost rate) of each product. The results show that the higher exergy destruction rate is attributed to the solar collectors. In the same line, Calise et al. [15] carried out an exergetic and exergoeconomic analysis of a hybrid solar geothermal multi-generation system, equipped with an organic Rankine cycle driven by parabolic trough solar collectors and a geothermal well, where a multi-effect distillation unit and an absorption chiller are coupled to the power block. The exergoeconomic accounting method was applied to calculate all the energy and material output costs, comparing on a daily, weekly and annual basis, which allows evaluating the performance of the system and the variability observed during the year. Alternatively, Ortega et al. [16] presented a thermoeconomic analysis with the integration of seawater desalination processes coupled to a CSP plant, as well as its comparison with stand-alone plants such as multi-effect distillation (MED) and reverse osmosis. The evaluation considered the unit exergy cost of electricity and water. The results showed that the best coupling scenario for CSP-MED configurations was replacing the condenser of the CSP plant by a MED system. Furthermore, the increase on the fresh water production caused a reduction on the water cost. In this context, in a previous publication by the authors Leiva-Illanes et al. [4], firstly it was carried out a thermoeconomic assessment of a solar polygeneration plant for producing four products (electricity, fresh water, cooling, and heat) in high direct normal irradiation conditions. Integration of a CSP plant, a MED unit, a single effect absorption chiller (REF), and a process heat (PH) module was analyzed in three configurations, two CSP-polygeneration schemes and one considering stand-alone systems. The plants were evaluated by applying the Bejan et al. method [7], comparing the unit exergy cost and exergy cost rate of the final products on an annual basis. That study revealed that the solar polygeneration plant evaluated was more efficient and cost-effective than the stand-alone plants in zones with high irradiation conditions and proximity to consumption centers, such as the Atacama Desert. In another study conducted by the authors Leiva-Illanes et al. [5], the levelized cost method and the thermoeconomic method were applied to the same solar polygeneration plant to analyze and compare the cost allocation process, the unit specific costs of products, the energy and exergy efficiencies, as well as the main advantages of each method. Through the levelized cost method, the cost associated to the electricity generation was higher than that one found with the thermoeconomic method, whereas the costs of water, cooling and process heat were significantly lower. Those results showed that the thermoeconomic method was an equitable and rational cost allocation method in that solar polygeneration plant based on CSP. Moreover, Mehrpooya et al. [17] a CSP plant with parabolic dish collectors and steam turbine, a multi-effect desalination plant, and a single-stage ammonia-water absorption refrigeration system was developed and assessed through exergy analysis. The annualized cost of system method was employed to perform the economic analysis of the proposed integrated system. The results of the economic analysis showed that the proposed integrated structure had a positive net present value and attractive rate of return. Wellmann et al. [18] a cogeneration CSP plant tower considering the integration of a low temperature desalination plant, which was analyzed using an exergoeconomic method and the lost-kilowatts method. The plant was located on the Red Sea coast in Egypt. Two operational cases were examined, in which the water output and the electricity output were maximized, respectively. In the first case, the unit exergy cost of electricity was lower, while in the second case, the unit exergy cost of water was lower. However, the results showed that the electricity cost was not competitive to fossil fuel power plants. In a recent study of our group [19], a thermoeconomic analysis of a solar polygeneration plant for the joint production of electricity, fresh water, cooling, and process heat was carried out to analyze the process of exergy cost formation and compare it with stand-alone systems. In that study only one polygeneration configuration was analyzed. The results show that the main components that contribute to the costs formation are solar collectors, evaporator, re-heater, economizer, turbine, and super-heater. Also, a solar polygeneration plant is more cost effective than stand-alone systems. The present article constitutes the continuation of that research line, in which an exergy cost assessment in stand-alone systems and solar multi-generation schemes (including cogeneration, trigeneration, and polygeneration) is carried out considering the CSP plant as the prime mover and its integration with technologies driven by thermal energy for producing electricity, desalted water, cooling, and process heat. The CSP plant analyzed consists of a solar field with parabolic trough collectors, a thermal energy storage system, a power block, and a backup energy system. While the technologies driven by thermal energy consist of a multi-effect distillation plant, a single-effect LiBr-H_2O absorption refrigeration plant, and a countercurrent heat exchanger module. These technologies were selected because they are commercially available and allow operating within temperature ranges of the coupling points in the CSP plant. These points were selected according to the operating temperature constraints, imposed by each technology and aiming to cause the minimum penalty in terms of power production.

As mentioned above, different studies have applied the thermoeconomic method to analyze the integration of the CSP plant into multi-generation schemes. Those were mainly focused on the final cost of each product [3–5,15–18]. However, such studies did not consider the evaluation of the process of exergy cost formation, the analysis, comparison, and selection among configurations from stand-alone systems to solar schemes of cogeneration, trigeneration, and polygeneration. The exergy cost assessment, as Symbolic Exergoeconomic methodology [9], would allow to select the best configurations and identify potential improvement measures because it provides a more detailed information about the exergy cost formation process, the cost decomposition of each exergy cost, and the residue cost allocation. The process of exergy cost formation is crucial for the integration of complex thermal systems since it enables determining where the savings on resources could be found, and in turn identifying which specific components should be improved. Therefore, in the present study, the symbolic exergoeconomic method is applied to solar multi-generation schemes, as well as to stand-alone systems. The aim is to analyze and compare the process of exergy cost formation, determine the key equipment which could be candidates for improving its design, detect potential energy savings and establish the best configuration in each of these schemes, in terms of unit exergy cost of the product, total exergy cost of product, and exergy efficiency. The results of this study provide useful information to decision-makers, that could be used to improve the design and rational use of the energy resources in solar multi-generation systems and could constitute a guide to understand the process of cost formation in solar multi-generation schemes.

2. Methodology

The present article considers a thermodynamic simulation procedure for modelling and evaluating the performance of multi-generation plants. First, stand-alone systems are modelled and validated against data reported in the technical literature. Then the models of those stand-alone systems are evaluated by integrating them in different solar multi-generation schemes, in which a concentrated solar power plant is considered as the prime mover. Multi-generation plants are configured considering different coupling points to operate in cogeneration, trigeneration, and polygeneration schemes. Validation of the cogeneration, trigeneration, and polygeneration schemes is arranged by the combination of the validated stand-alone systems because currently there are not solar multi-generation plants of these characteristics in operation. The symbolic exergoeconomic methodology [9,20,21] is applied, which is based on the exergy cost theory [22]. An aggregation level is selected for each physical structure to define the boundaries of the analysis. Then, the productive structure is determined, in which fuel and product streams are established. The model assesses the overall efficiency of the systems and uses variables such as fuel, product, exergy cost and exergy efficiency of each system component. After that, the thermoeconomic model is solved. The main parameters to analyze are the unit exergy cost of each product, their cost formation process, the total exergy cost of product, and the exergy efficiency. Additionally, it is possible to analyze the influence of the individual consumption of each component on the total amount of external resources required to obtain a product.

2.1. Stand-alone systems

The CSP plant analyzed herein is depicted in Fig. 1, which is similar to the configuration of Andasol-1 power plant, located in Granada, Spain [23,24]. The CSP plant consists of a solar field (SF) with parabolic trough collectors, a thermal energy storage system (TES), a power block, and a backup energy system (BS) [23,25]. The SF is composed of EuroTrough collectors, Schott PRT- 70 absorber tubes, and Dowtherm A as heat thermal fluid. The design temperature of the SF is of 393 °C and 293 °C as the outlet and inlet temperature. The direct normal irradiance and solar collector efficiency at design point (21st December solar noon at Crucero, Chile) are 1 010 W/m^2 and 0.72, respectively. The solar field aperture area is defined as 510 120 m^2, equivalent to the design point of Andasol-1, leading to a solar multiple of 2.56. The TES consists of a two-tank indirect system using molten salts as storage media, and with a design temperature of 386 °C and 292 °C for the hot and cold tanks, respectively. TES was designed to cover 12 h of continuous operation. The power block consists of a regenerative Rankine cycle with reheat and six extractions, as described by Blanco-Marigorta et al. [25]. The gross power is 55.0 MW_e, the high-pressure turbine inlet pressure is 100.0 bar and the low-pressure turbine backpressure is 0.06 bar. The high and low-pressure turbines have isentropic efficiencies of 85.2% and 85.0%, respectively. The generator efficiency is considered as 98.0%, and pumps' isentropic efficiency is 70.0%.

The size of the plants has been established to satisfy a large-scale supply from the mining industry, such as observed in northern Chile, Australia, and North-Africa, which operates continuously and consequently presents a constant demand.

Figs. 2–4 show the configuration of the thermal driven cycles analyzed herein. Each figure represents a simplified physical structure of each stand-alone scheme. Each system is fueled by natural gas (stream 1) to generate heat in the boiler (streams 2 and 3), where this thermal energy drives the multi-effect distillation, single-effect absorption refrigeration, and process heat module respectively. The electricity supplied from the Grid is represented by the Grid module that considers a combined cycle power plant. Additionally, it is considered a dissipative device in the case of the MED and REF; its purpose is to conveniently assess the costs of the residues generated.

Fig. 2 shows the MED plant that consumes steam from the boiler (streams 2 and 3), seawater (stream 5), and electricity (stream 4) from the Grid. The MED plant generates fresh water (stream 6) and presents two residues: the cooling seawater (Stream 7) and the brine (stream 8). The desalination plant is modelled considering 12 effects, parallel-cross feed and 11 feed preheaters, as suggested by Zak et al. [26]. The feed seawater intake temperature is considered at 25 °C and its salinity as 0.042 kg/kg; the feed seawater temperature after down condenser is established at 35 °C and the maximum salinity at each effect is 0.072 kg/kg. The top brine temperature is 65 °C, and the concentrate factor is estimated as 1.7. Then, the Gained Output Ratio determined according to the operation condition is 9.1, which is defined as the mass ratio between the distillate produced and the steam supplied to the system, while the specific heat consumption is 245.2 kJ/kg, the specific electricity consumption is 1.5 kWh/m^3, and the fresh water production is 430.2 kg/s (37 168 m^3/day).

Fig. 3 depicts a stand-alone REF plant, driven by the thermal energy from the boiler (streams 2 and 3) and consuming electricity from the Grid (stream 4). The REF plant generates chiller water (stream 5) and the cooling water (streams 6 and 7) is considered as residue. The refrigeration plant is configured by a single-effect LiBr-H_2O absorption chiller, which is modelled as described by Herold et al. [27]. It has a cooling capacity of 5 MW_{th} (1 421.73 tons) and a nominal coefficient of performance of 0.7 [27]. The chilled water inlet and oultlet temperatures are 10 °C and 6 °C, respectively, while the inlet and outlet cooling water temperatures are 25 °C and 35 °C, respectively. Finally, the heat medium operating temperature is 108.5 °C.

Respecting the stand-alone PH plant, Fig. 4 shows its configuration where the module receives thermal energy from the boiler (streams 2 and 3) and electricity from the Grid (stream 4). A countercurrent shell-and-tube heat exchanger is configured to deliver a thermal load of 7 MW_{th} of heating (stream 5). The heat exchanger inlet and outlet temperatures are 63 °C and 90 °C respectively.

The thermodynamic modelling of these stand-alone plants were validated by comparing simulations results with the reference cases. The power cycle was validated at the design point using the data of Andasol-1 reported by Blanco-Marigorta et al. [25]. Furthermore, the CSP plant was also validated by comparing the results between the IPSEpro/Matlab model and the case study (Andasol-1) by means of the SAM software [23]. The results indicate differences of 3.6% in terms of annual net electricity, and 1.5% in thermal efficiency. Related to the MED plant, it was validated considering the data reported by Zak et al. [26] and from El-Dessouky et al. [28]. The results show no differences in the total distillate water production, 5.46% error in terms of specific heat transfer area, and 7.81% regarding the Gained Output Ratio. Finally, the thermodynamic model of the REF plant was validated using the data reported by Herold et al. [27]. The results show differences

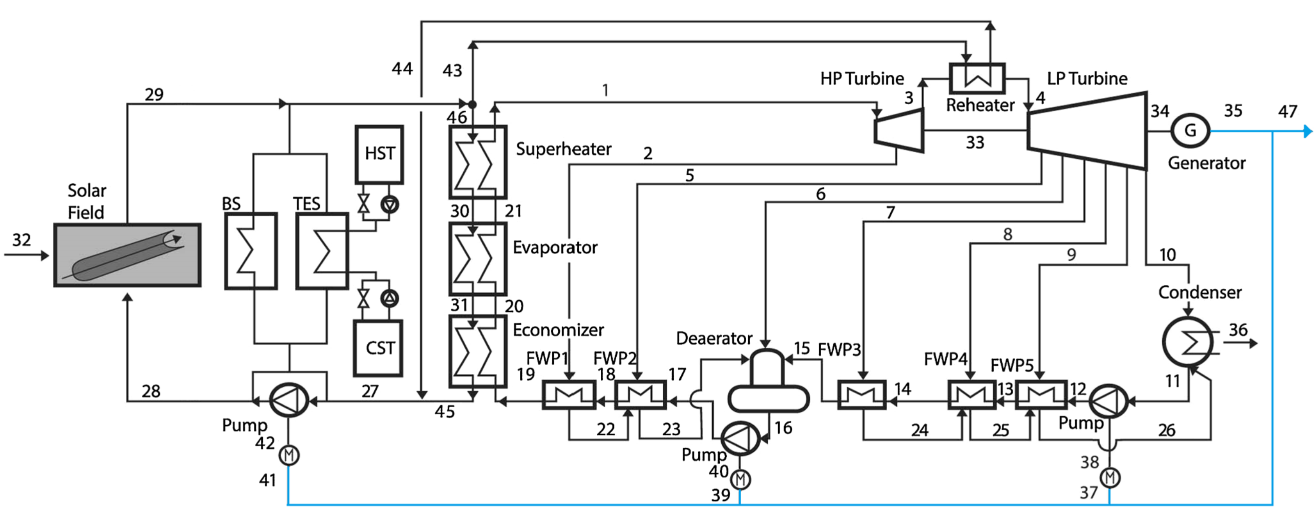

Fig. 1. Configuration of the stand-alone CSP plant (physical structure of the system). CST: cold storage tank, FWP: feed water preheater, G: generator, HP: high pressure, HST: hot storage tank, LP: low pressure.

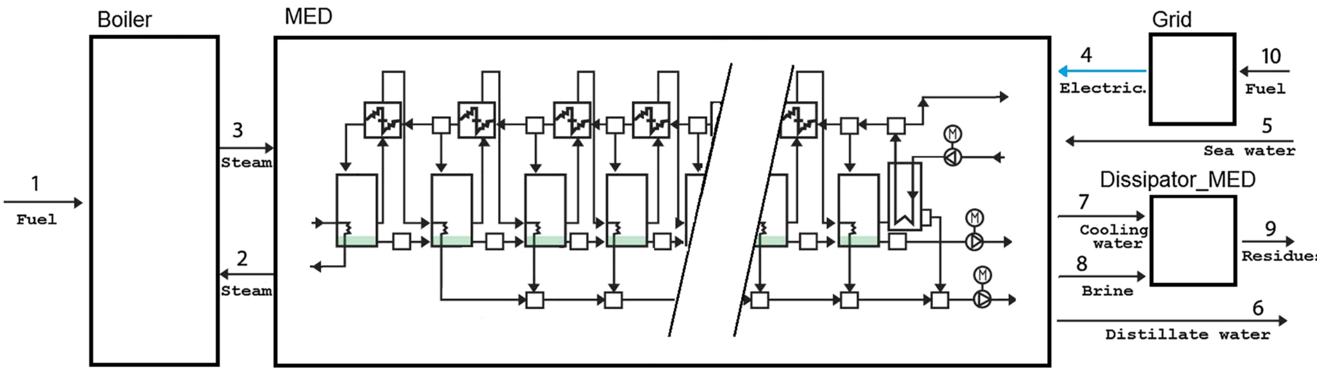

Fig. 2. Configuration stand-alone MED plant (simplified physical structure of the system).

lower than 2.6% in terms of the cooling capacity and COP.

2.2. Multi-generation schemes

Different options of coupling points into the CSP plant are depicted in Fig. 5. Each plant (MED, REF, and PH) is coupled in different locations in order to analyze, compare, and obtain the best configurations in the solar multi-generation schemes (cogeneration, trigeneration, and polygeneration).

In the MED plant, two coupling points are considered due to the first effect of the MED plant must operate within a temperature range of 64–74 °C [29]. The first configuration considers the MED plant substituting the condenser of the power cycle, leading to a modification on the turbine back pressure from 0.06 to 0.37 bar. Hence, to keep the gross power, the solar field aperture area is increased, besides, if the MED plant is coupled to the sixth turbine extraction, it is not necessary to modify the turbine back pressure, yet the solar field aperture area should also be increased, to keep the same gross power output. Regarding the fresh water production, when the MED plant replaces the power cycle condenser, it is not possible to regulate the production independently because it depends on the electricity production. In the second configuration the production can be regulated, assuming a design point of 300 kg/s. In general, when any plant replaces the condenser of the power cycle, it is not possible to modify the production because the condenser operates according to the conditions of the power cycle.

In the case of the REF plant, two coupling points are considered, in which the desorber of the single-effect absorption refrigeration plant should operate between 80 and 110 °C [30]. When the REF plant is coupled to the 5th turbine extraction, it is not necessary to modify the turbine back pressure, but the solar field aperture area must also be increased, to keep equivalent power output. Conversely, if the REF plant is coupled to the 6th turbine extraction, the turbine back pressure is modified from 0.06 to 0.37 bar, and the solar field aperture area must be increased. Note that it is not recommended that the REF plant replaces the condenser of the power cycle because the higher turbine back pressure would mean an important penalty in power block's efficiency. Respecting the cooling production, it can be modified according to the demand in both configurations.

About the PH plant, four configurations are analyzed, in which the PH plant is coupled between feed water preheaters, in a turbine extraction, at the SF inlet, or at the SF outlet. In these cases, the turbine back pressure is not modified; however, the solar field should be increased, to deliver equivalent power output. The process heat production could vary depending on the demand in all configurations, but those variations would not affect the design point of the cogeneration plant.

The output of any product is dependent on the operating parameters of the CSP plant. When the production of any product is reduced, the power cycle needs less energy input to generate the nominal power output, and the control system could either reduce the energy input to the power cycle by partial defocusing solar collectors, or reducing the thermal energy output from TES and/or backup system.

Different multi-generation schemes are configured as listed in Table 1, where the coupling points mentioned are related to the stand-alone CSP configuration. The turbine back pressure is modified only when the MED plant replaces the condenser, and in all the schemes analyzed the size of the solar field is increased to maintain the same power output. The production of fresh water is adjusted to the production of electricity when the condenser is replaced by the MED plant but in the other case, it is fixed. Twenty-one case studies are analyzed, twenty of them regarding solar multi-generation plants: eight of cogeneration (CSP-MED, CSP-REF, and CSP-PH), eight of trigeneration (CSP-MED-REF, CSP-REF-PH, and CSP-MED-PH), four polygeneration

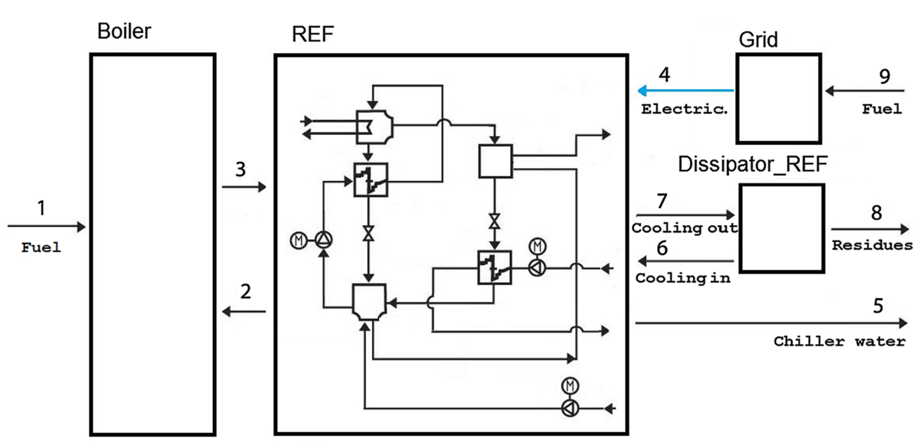

Fig. 3. Configuration stand-alone REF plant (physical structure of the system).

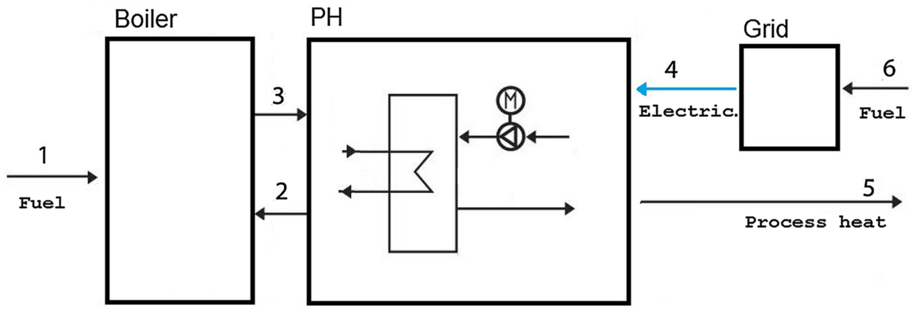

Fig. 4. Configuration stand-alone PH plant (physical structure of the system).

schemes (CSP-MED-REF-PH), and the twenty-first considering stand-alone systems. These case studies illustrate different potential configurations to be installed in zones with high direct normal irradiation conditions.

The size of each plant for all multi-generation configurations (cogeneration, trigeneration, and polygeneration) is: 55 MW_e, 300 kg/s, 5 MW_{th}, and 7 MW_{th}, for the CSP, MED, REF, and PH plants, respectively. Only in the case that the MED plant replaces the condenser, water production capacity would be different since its production depends on the amount of energy that is rejected in the thermodynamic power cycle.

On the polygeneration schemes, the first configuration named Poly 1 is depicted in Fig. 6a, where the MED plant replaces the condenser on stream 10, the REF plant is coupled to the 6th turbine extraction on stream 9, and the PH plant is coupled between FWP3 and FWP4 on stream 14. The second scheme called Poly 2 and depicted in Fig. 6b considers the MED plant coupled to the 6th turbine extraction on stream 9, the REF plant coupled to the 5th turbine extraction on stream 8, and the PH plant coupled between FWP3 and FWP4 on stream 14. The third one, Poly 3, is shown in Fig. 6c; it is similar to Poly 1 except that the PH plant is coupled to the 5th turbine extraction on stream 8. Finally, Poly 4 is depicted in Fig. 6d, which is analogous to Poly 2, but the PH plant is coupled to the 4th turbine extraction on stream 7. Poly 1 and Poly 2 were analyzed in a previous study conducted by the authors [4] focusing on determining the actual cost of each product and establishing the effect of investment, fuel cost, demand, and sizing of the SF and TES in polygeneration plants. Poly 1 was also used in the previous paper [5] to compare the levelized cost method [31] and the thermoeconomic method [7].

The performance of the solar multi-generation schemes was evaluated, considering the features established by the design point, and considering the data of a meteorological year [32] in a high solar irradiation area. Software IPSEpro [33] was employed for modelling and simulating the different systems, were the IPSEpro-MDK and IPSEpro-PSE modules were used. IPSEpro-MDK is a programming environment that offers all the capabilities required to define and build new component models in an existing library or the creation of a new library, and to translate them into a language interpretable by IPSEpro-PSE. IPSEpro-PSE is a process simulation environment that allows establishing mass and energy balances, simulating different kinds of processes, through iterative Newton-Raphson method. The main advantage is the rapid convergence of the system, with an average calculation time of only few seconds. The simulation tool allows determining simulation of steady state operating conditions. Time-dependent phases in plant operation can be simulated using IPSEpro-PSXLink, that allows integrating IPSEpro-PSE projects with Microsoft Excel. The exergoeconomic evaluation was conducted using MATLAB and the ExIO module [34] as a complement of the Microsoft Excel.

2.3. Exergoeconomic method

The symbolic exergoeconomic methodology [9,20,21] was applied, which is based on the exergy cost theory (ECT) [22]. The method provides a general criterion that enables to assess the efficiency of energy systems and rationally explains the process of cost formation of products. Thus, it is a cost accounting methodology that proposes methods to determine the number of resources required for delivering a specific product. The cost formation process can be easily obtained by using matrix algebra. The exergy cost theory requires a mathematical modelling of the physical and productive structure of the system. This last structure is built according to the purpose of each component and shows the origin of the resources of each component and its products.

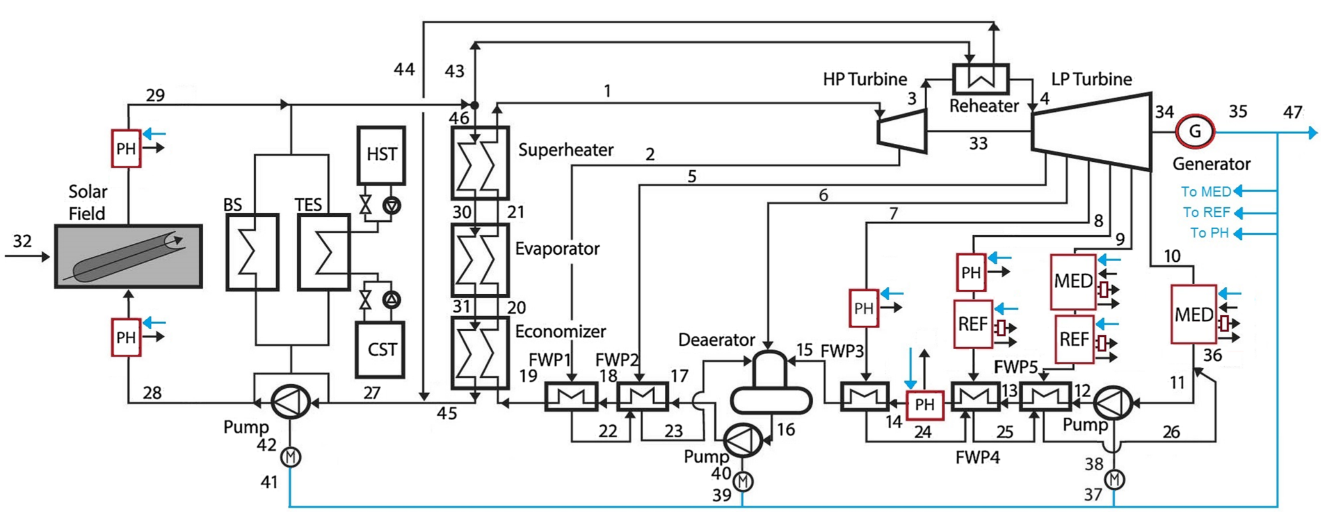

Fig. 5. Coupling points into the CSP plant analyzed in multi-generation schemes.

Table 1
Stand-alone systems and solar multi-generation schemes.

	Coupling point in CSP plant	Turbine back P bar	Aperture area m^2	Fresh water kg/s
Stand-alone systems	–	0.06	510 120	430.2
Cogeneration				
Cogen 1 (CSP-MED 1)	MED replaces the condenser	0.37	598 452	466.4
Cogen 2 (CSP-MED 2)	MED in 6th extraction	0.06	575 202	300.0
Cogen 3 (CSP-REF 1)	REF in 5th extraction	0.06	520 861	–
Cogen 4 (CSP-REF 2)	REF in 6th extraction	0.37	604 748	–
Cogen 5 (CSP-PH 1)	PH between FWP3-FWP4	0.06	523 991	–
Cogen 6 (CSP-PH 2)	PH in 5th extraction	0.06	520 691	–
Cogen 7 (CSP-PH 3)	PH before collectors in SF	0.06	535 161	–
Cogen 8 (CSP-PH 4)	PH after collectors in SF	0.06	535 169	
Trigeneration				
Trigen 1 (CSP-MED-REF 1)	MED replaces the condenser, REF in the 6th extraction	0.37	603 721	443.6
Trigen 2 (CSP-MED-REF 2)	MED in the 6th extraction, REF in the 5th extraction	0.06	585 316	300.0
Trigen 3 (CSP-REF-PH 1)	REF in the 5th extraction, PH in the 4th extraction	0.06	533 768	–
Trigen 4 (CSP-REF-PH 2)	REF in the 5th extraction, PH between FWP3-FWP4	0.06	533 716	–
Trigen 5 (CSP-MED-PH 1)	MED replaces the condenser, PH between FWP3-FWP4	0.37	611 378	453.0
Trigen 6 (CSP-MED-PH 2)	MED in the 6th extraction, PH between FWP3-FWP4	0.06	588 390	300.0
Trigen 7 (CSP-MED-PH 3)	MED replaces the condenser, PH in the 5th extraction	0.37	607 282	448.2
Trigen 8 (CSP-MED-PH 4)	MED in the 6th extraction, PH in the 5th extraction	0.06	585 151	300.0
Polygeneration				
Poly 1	MED replaces the condenser, REF in the 6th extraction, PH between FWP3-FWP4	0.37	616 650	430.2
Poly 2	MED in the 6th extraction, REF in the 5th extraction, PH between FWP3-FWP4	0.06	598 510	300.0
Poly 3	MED replaces the condenser, REF in the 6th extraction, PH in the 5th extraction	0.37	612 558	425.4
Poly 4	MED in the 6th extraction, REF in the 5th extraction, PH in the 4th extraction	0.06	598 573	300.0

Each plant has only one physical structure to describe the physical relations between the process units, but various productive structures can be defined depending on the fuel and product definitions as well as the disaggregation level selected. The disaggregation level is interpreted as the degree of accuracy of the analysis. Each subsystem can be part of an equipment, an equipment itself, or a group of equipment. The productive diagram is a graphic representation of the thermoeconomic model of the plant, in which the inputs of a component are its resources, and the outputs of a component are its products. This structure is composed of n components connected by flows, which are characterized by their exergy. Each component consumes resources from other components or from the environment (those resources are denominated Fuel), to produce useful effects for other components or for the environment (those useful effects are named Product). Fuel (F) is partially transformed into product (P) and partially destroyed as irreversibility (I). A flow from component i to component j is represented by the exergy flow, then, the Fuel and Product is defined as:

$$F_i = P_i + I_i = \sum_{j=0}^{n} E_{ji} \tag{1}$$

$$P_i = F_i - I_i = \sum_{j=0}^{n} E_{ij} \tag{2}$$

where E_{ij} is the exergy flow, the subscripts i and j denotes generic components.

The fuel-product presentation is the adjacency matrix of the productive graph, that allows getting all flows within the productive structure, and is based on distribution coefficients y_{ij} which indicate the proportion of the production of the j-th component used as resource for the i-th component. It shows how the product of a component is distributed among the other components and the environment.

$$y_{ij} = \frac{E_{ji}}{P_j} \tag{3}$$

Expressing the Eq. (1) as function of y_{ij}, it yields:

$$F_i = E_{0i} + \sum_{j=1}^{n} E_{ji} = E_{0i} + \sum_{j=1}^{n} y_{ij}\cdot P_j \tag{4}$$

The previous equation in matrix notation is:

$$\boldsymbol{F} = \boldsymbol{F_e} + \langle \boldsymbol{FP} \rangle\cdot \boldsymbol{P} \tag{5}$$

where $\boldsymbol{F}$ and $\boldsymbol{P}$ are vectors of all fuels and products, $\boldsymbol{F_e}$ is the vector of external resources, and $\langle \boldsymbol{FP} \rangle$ is a matrix composed of elements y_{ij}.

Similarly, with the same procedure, it is obtained:

$$\boldsymbol{P} = (\boldsymbol{K_D} - \langle \boldsymbol{FP} \rangle)^{-1}\cdot \boldsymbol{F_e} \tag{6}$$

where $\boldsymbol{K_D}$ is a diagonal matrix containing the unit exergy consumptions of all components (k_j), defined as:

$$k_j = \frac{F_j}{P_j} = \frac{1}{\psi_j} \tag{7}$$

where ψ_j is the exergy efficiency (ratio between the exergy rate of product and the exergy rate of fuel) that is an efficiency based on the Second-Law of Thermodynamics and weights energy and matter flows by accounting for each in terms of exergy.

Eq. (6) allows calculating the products of all components starting from the external resources consumed by the plant ($\boldsymbol{F_e}$), using the parameters that define the components (unit exergy consumptions and distribution coefficients).

The unit exergy cost of a flow c_{ij} is the relation between its exergy cost C_{ij} and its exergy, where C_{ij} is the amount of exergy resources consumed by that system used to produce this flow.

$$c_{ij} = k_{ij}^{*} = \frac{C_{ij}}{E_{ij}} \tag{8}$$

In thermoeconomic analysis, energy systems, such as multi-generation plants, could present productive and dissipative components. The productive components provide functional products, fuel (resources) to other processes, as well as residues and waste disposals. Likewise, the dissipative components are required to reduce or eliminate the environment impact of residues and waste, to maintain the operating conditions of the system and improve its efficiency.

According to the cost model, the exergy cost of the product is defined as:

$$C_{P,i} = C_{F,i} + C_{R,i} \tag{9}$$

where C is the exergy cost, and the subscripts P, F, and R mean

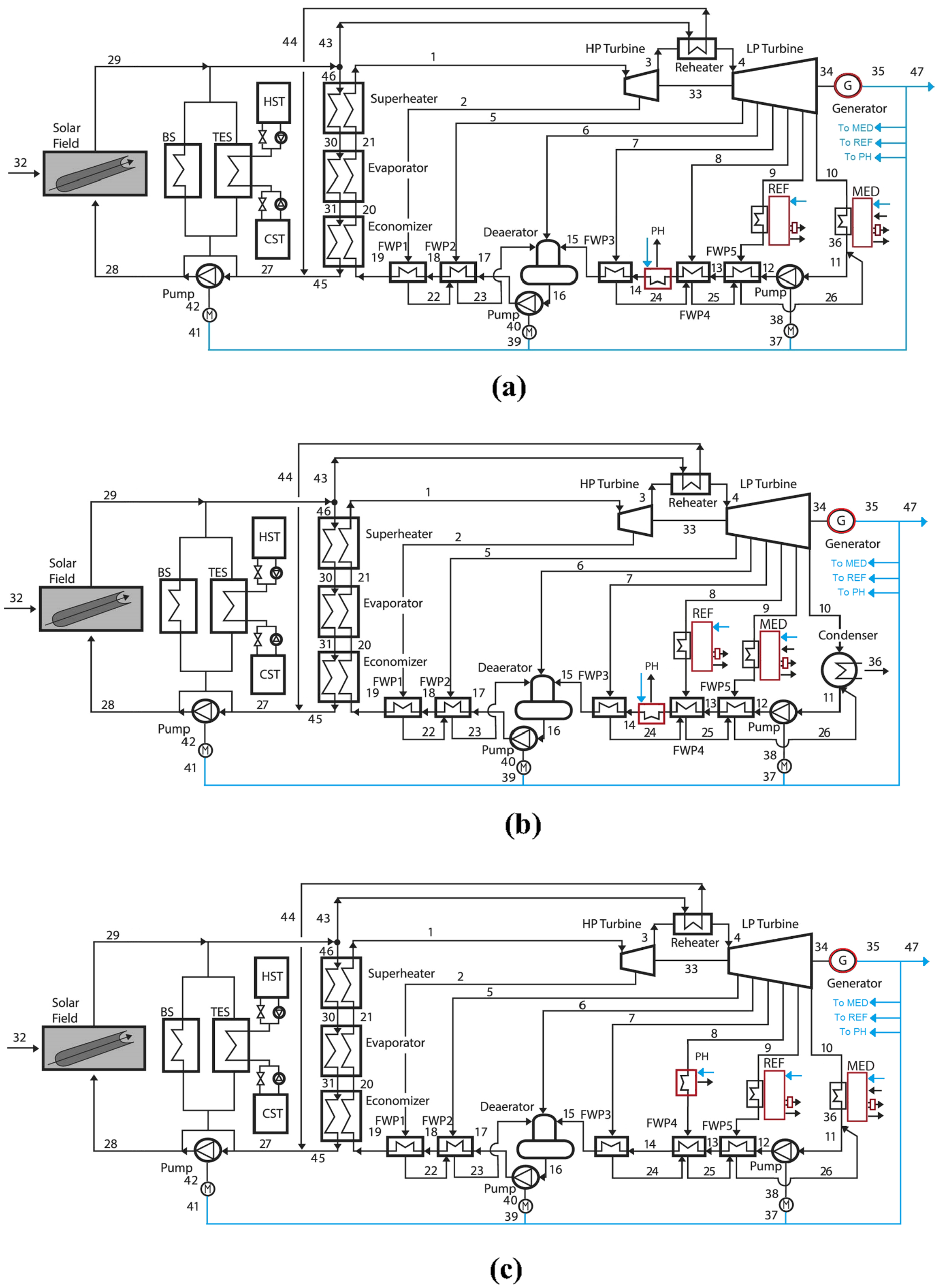

Fig. 6. Configuration CSP-polygeneration schemes. (a) Poly 1, (b) Poly 2, (c) Poly 3, (d) Poly 4.

product, fuel, and residues, respectively.

The exergy cost of product represents the resources required (in exergy rate units) to carry out the production, for instance, an exergy cost of electricity of 193 476 kW means that 193 476 kW of exergy of resources are needed for producing 55.0 MW_e of electricity.

The costs of the external resources are known values as:

$$C_{e,i} = E_{0i} \tag{10}$$

and the cost of each flow making up the product is proportional to its exergy:

$$C_{ij} = c_{P,i} \cdot E_{ij} \tag{11}$$

where $c_{P,i}$ is the unit exergy cost of the product of i-th component.

The unit exergy cost of product represents the amount of exergy

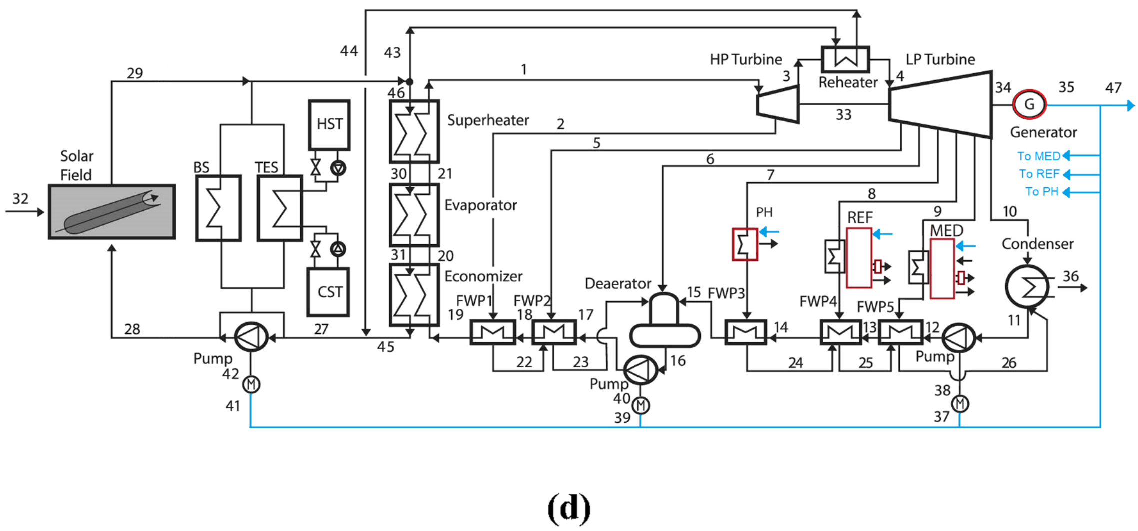

Fig. 6. (*continued*)

Table 2
Fuel-Product definition of the stand-alone CSP plant.

	Component	Fuel	Product
0	Environment	$E_{47} + E_{36}$	E_{32}
1	Collectors	E_{32}	$E_{29} - E_{28}$
2	Pump1	E_{42}	$E_{28} - E_{27}$
3	Motor1	E_{41}	E_{42}
4	Economizer	$E_{31} - E_{45}$	$E_{20} - E_{19}$
5	Evaporator	$E_{30} - E_{31}$	$E_{21} - E_{20}$
6	Superheater	$E_{46} - E_{30}$	$E_{1} - E_{21}$
7	Reheater	$E_{43} - E_{44}$	$E_{4} - E_{3}$
8	HP_Turbine	$E_{1} - E_{2} - E_{3}$	E_{33}
9	LP_Turbine	$E_{4} - E_{5} - E_{6} - E_{7} - E_{8} - E_{9} - E_{10} + E_{33}$	E_{34}
10	Generator	E_{34}	E_{35}
11	Pump3	E_{38}	$E_{12} - E_{11}$
12	Motor3	E_{37}	E_{38}
13	FWP5	$E_{9} + E_{25} - E_{26}$	$E_{13} - E_{12}$
14	FWP4	$E_{8} + E_{24} - E_{25}$	$E_{14} - E_{13}$
15	FWP3	$E_{7} - E_{24}$	$E_{15} - E_{14}$
16	Deaerator	$E_{6} + E_{15} + E_{23}$	E_{16}
17	Pump2	E_{40}	$E_{17} - E_{16}$
18	Motor2	E_{39}	E_{40}
19	FWP2	$E_{5} + E_{22} - E_{23}$	$E_{18} - E_{17}$
20	FWP1	$E_{2} - E_{22}$	$E_{19} - E_{18}$
21	Node1	$E_{44} + E_{45}$	E_{27}
22	Node2	E_{29}	$E_{43} + E_{46}$
23	Node3	E_{35}	$E_{47} + E_{37} + E_{39} + E_{41}$
24	Condenser	$E_{10} - E_{11} + E_{26}$	E_{36}

required to get a unit of exergy of the product, i.e. the resources required to carry out the production. For instance, a unit of exergy cost of electricity of 3.51 kW/kW means that 3.51 kW of exergy of resources are needed for producing 1 kW of electricity.

Note that the exergy cost and the unit exergy cost allow measuring in the same unit resources and products of different nature, such as electricity, water, cooling, process heat, resources, and waste.

Regarding to the production cost decomposition, the exergy cost of the product is decomposed into two parts:

$$\boldsymbol{C}_P = \boldsymbol{C}_P^e + \boldsymbol{C}_P^r \tag{12}$$

where $\boldsymbol{C}_P^e$ is the exergy cost due to irreversibilities of the components (the sum of the irreversibilities accumulated along the process) and $\boldsymbol{C}_P^r$ is the exergy cost due to the residues allocation. Eq. (12) includes the exergy cost irreversibilities relationship in implicit form. In this equation the residue costs are considered and accounted as external irreversibilities.

In the same way, the unit exergy cost of the product is decomposed into two parts, the unit production cost due to irreversibilities of the components and the unit production cost due to the residues; where the unit exergy cost is expressed in kW/kW. The detailed formulation of the Symbolic Exergoeconomic methodology is described in more details in [19,21,35]. Summarizing, the process to assess the cost of the flow streams and processes in a multi-generation plant helps to understand the process of cost formation, from the input resources to the final products. Note that $\boldsymbol{c_p}$ and $\boldsymbol{C_p}$ can be transformed into economic costs expressed in USD/kWh and USD/h, respectively. The validity of the method is maintained if investment and operation costs are considered [35]. Then, production costs can be broken down into three contributions: the cost of the resources needed to obtain it (due to the irreversibilities of the components), non-thermodynamic costs (due to the investment and operation costs), and waste (residues). This analysis was already carried out by the authors in two previous studies [4,5] to Poly 1 and Poly 2 schemes, as well as to stand-alone systems.

In the present analysis, different levels of disaggregation were taken: for the CSP plant, it is considered at the level of components as shown in the physical structure in Fig. 1, and the systems providing by-products are considered at the level of a unique subsystem as depicted in Figs. 2–6. These considerations are due to the fact that the solar multi-generation plant was configured as a topping cycle, in which the priority is the production of electricity, while the by-products are generated according to the availability of thermal energy. Therefore, any failure or operation problem in the CSP plant affects the other plants (MED, REF, or PH) and not vice versa, unless one of those plants replaces the condenser of the power cycle.

Tables 2–5 show the Fuel-Product definition for the stand-alone systems. All the plants have productive and dissipative components, except the stand-alone PH plant that only has productive components. The dissipative components are the condenser in the CSP plant, the Dissipator_MED, and the Dissipator_REF. The purpose of the dissipative devices is to consider the residue generated (an output which is not considered as a product) in the productive unit. In this model, it is

Table 3
Fuel-Product definition of the stand-alone MED plant.

	Component	Fuel	Product
0	Environment	$E_{6} + E_{9}$	$E_{1} + E_{10} + E_{5}$
1	Boiler	E_{1}	$E_{3} - E_{2}$
2	MED	$(E_{3} - E_{2}) + E_{4} + E_{5}$	$E_{6} + E_{7} + E_{8}$
3	Grid	E_{10}	E_{4}
4	Dissipator_MED	$E_{7} + E_{8}$	E_{9}

Table 4
Fuel-Product definition of the stand-alone REF plant.

	Component	Fuel	Product
0	Environment	$E_5 + E_8$	E1 + E_9
1	Boiler	E_1	E_3-E_2
2	REF	E_3-E_2 + E_4	E_5 + (E_7-E_6)
3	Grid	E_9	E_4
4	Dissipator_REF	E_7-E_6	E_8

Table 5
Fuel-Product definition of the stand-alone PH plant.

	Component	Fuel	Product
0	Environment	E_5	$E_1 + E_6$
1	Boiler	E_1	$E_3 - E_2$
2	PH	$(E_3 - E_2) + E_4$	E_5
3	Grid	E_6	E_4

assumed that the residues leave a dissipative component, where all the abatement costs of these residues are charged (proportional to the cost of products dissipated). Note that the first row (Environment) contains the interactions between the system and the environment because the latter is also considered as a process.

Similarly, the same procedure of defining Fuel-Product streams is carried out for the cogeneration, trigeneration, and polygeneration schemes.

Once Fuel-Product streams are defined, the exergy rate of each flow must be calculated. The exergy rate of a matter flow can be expressed in terms of physical, chemical, kinetic, and potential component. While, the exergy rate of heat (E_Q) and work (E_W) are defined as

$$E_Q = \left(1 - \frac{T_0}{T_j}\right)\cdot\dot{Q}_j \quad (13)$$

$$E_W = \dot{W}_j \quad (14)$$

where T_0 is the temperature of reference, in K, $\dot{Q}$ is the heat transfer rate, and $\dot{W}$ is the work power. The subscripts Q, j, and W are the heat transfer, control volume, and work, respectively. The reference environment assumed is T_0 = 25 °C and P_0 = 1.013 bar. Similarly, the reference mass fraction of LiBr and water salinity is considered of 0.5542 kg/kg [36] and 0.042 kg/kg [37], respectively.

The exergy rate of fossil fuel is calculated with following relation [38]

$$E_{ff} = \dot{m}_{ff}\cdot\xi\cdot LHV \quad (15)$$

where ξ is an experimental correlation [38], LHV is the lower heating value of the fossil-fuel. The subscript ff denotes fossil-fuel.

$$\xi = 1.033 + 0.0169\cdot\frac{y}{x} - \frac{0.0698}{x} \quad (16)$$

where x and y are the composition C_xH_y in a general gaseous fuel. In the present article, the natural gas is considered as methane (CH_4).

The exergy rates of solar radiation are determinated by Petela‘s equation [39], which is one of the most cited models in the literature. It is defined as:

$$E_{sun} = A\cdot G_b\cdot\left(1 + \frac{1}{3}\left(\frac{T_0}{T_{sun}}\right)^4 - \frac{4}{3}\left(\frac{T_0}{T_{sun}}\right)\right) \quad (17)$$

where A is the solar field aperture area, G_b is the direct normal irradiance, and T_{sun} is the apparent temperature of the sun, taken as 6 000 K [39].

Other assumptions were adopted throughout the simulation process, as listed below:

- For stand-alone MED, REF, and PH plants, the unit exergy cost of the electricity from the Grid is assumed to be 2.44 kW/kW [20].
- Nominal conditions of all the configurations have been used to estimate the exergy costs.

3. Results and discussion

3.1. Comparison between stand-alone systems and multi-generation schemes

The results of stand-alone systems and solar multi-generation schemes in terms of the unit exergy cost of product (electricity, water, cooling, and heat), the total exergy cost of product, and the exergy

Table 6
Unit exergy cost, exergy cost, and exergy efficiency in stand-alone systems and solar multi-generation schemes.

	c_p electricity kW/kW	c_p water kW/kW	c_p cooling kW/kW	c_p heat kW/kW	C_p total kW	ψ_i %
Stand-alone systems	3.51	55.55	25.22	7.56	332 310	18.0
Cogeneration						
Cogen 1 (CSP-MED 1)	3.26	23.04	–	–	234 849	25.6
Cogen 2 (CSP-MED 2)	3.39	23.86	–	–	223 294	26.3
Cogen 3 (CSP-REF 1)	3.50	–	15.07	–	197 379	28.6
Cogen 4 (CSP-REF 2)	4.08	–	17.64	–	230 226	24.7
Cogen 5 (CSP-PH 1)	3.51	–	–	5.11	198 533	28.8
Cogen 6 (CSP-PH 2)	3.50	–	–	4.49	197 266	29.0
Cogen 7 (CSP-PH 3)	3.52	–	–	8.34	202 679	28.2
Cogen 8 (CSP-PH 4)	3.50	–	–	9.36	202 641	28.2
Trigeneration						
Trigen 1 (CSP-MED-REF 1)	3.28	22.66	13.74	–	236 567	25.4
Trigen 2 (CSP-MED-REF 2)	3.39	23.37	14.59	–	227 182	26.0
Trigen 3 (CSP-REF-PH 1)	3.48	–	15.02	5.73	202 249	28.4
Trigen 4 (CSP-REF-PH 2)	3.50	–	15.07	5.01	202 254	28.4
Trigen 5 (CSP-MED-PH 1)	3.29	22.79	–	5.02	239 666	25.4
Trigen 6 (CSP-MED-PH 2)	3.39	23.41	–	5.47	228 423	26.2
Trigen 7 (CSP-MED-PH 3)	3.27	22. 67	–	5.12	237 949	25.6
Trigen 8 (CSP-MED-PH 4)	3.39	23.40	–	4.35	227 189	26.3
Polygeneration						
Poly 1	3.29	22.77	13.78	5.07	241 306	25.3
Poly 2	3.38	23.34	14.54	5.28	232 165	25.9
Poly 3	3.27	22.66	13.71	5.13	239 593	25.5
Poly 4	3.38	23.32	14.53	5.47	232 175	25.9

efficiency are shown in Table 6.

The stand-alone CSP plant was analyzed considering a turbine back pressure of 0.06 bar. This condition is modified, for example, when the MED plant replaces the power cycle condenser as in some configurations of multi-generation schemes. In this context, if the turbine back pressure is set to 0.37 bar in a stand-alone CSP plant, the unit exergy cost of electricity would be increased to 4.14 kW/kW (17.9% more expensive). Clearly, the turbine back pressure is an important parameter that strongly influences power cycle performance. On the other hand, the unit exergy cost of electricity in the stand-alone CSP plant is higher than in the multi-generation schemes, except in the cases of Cogen 4 (CSP-REF 2) and Cogen 7 (CSP-PH 3), in which the turbine back pressure is 0.37 bar and the PH coupling point is in the solar field, respectively. Cogen 4 (CSP-REF 2) negatively affects the efficiency of the power cycle, while in Cogen 7 (CSP-PH 3) the temperature difference between the cold stream to be heated up (the process stream) and the hot stream (the heat source) is high, then exergy destruction is also high. The other stand-alone plant (MED, REF, and PH) are coupled to a boiler, which also has a high exergy destruction. The main reason for the high exergy destruction in the boiler (combustion chamber) are the chemical reactions and heat exchange between streams with large temperature differences [5,40]. Consequently, the unit exergy cost of water, cooling, and heat in the stand-alone plant are higher than in solar multi-generation schemes, except in the cases of Cogen 7 (CSP-PH 3) and Cogen 8 (CSP-PH 4), which are coupled in the solar field. The high exergy destruction is explained due to the large temperature difference between the source temperature and the heat transfer fluid. The comparison between stand-alone systems and polygeneration schemes are presented in Fig. 7. Poly 3, the best configuration of all polygeneration schemes, allows reducing the unit exergy cost by 6.8%, 59.2%, 45.6%, and 32.2% for electricity, water, cooling, and process heat, respectively.

The total exergy cost of products in stand-alone systems is higher than solar polygeneration schemes; however, they can only be compared if they present the same capacity [4]. Consequently, they are compared to Poly 1. The total exergy cost of the stand-alone systems is distributed as 58.2%, 37.0%, 2.4%, and 2.3% in electricity, water, cooling, and process heat, respectively. While in Poly 1, it is distributed as 75.1%, 20.9%, 1.8%, and 2.2%, correspondingly. Therefore, in terms of exergy cost, the main impact is reflected in the electricity production, followed by the water production. Regarding the exergy efficiency, the stand-alone systems have lower efficiency than the solar multi-generation schemes, meaning that the solar multi-generation systems consider a more rational use of resources. Finally, according to the comparison between stand-alone systems and multi-generation schemes, the results show that the solar multi-generation schemes are more cost-effective than stand-alone systems. Additionally, the solar multi-generation schemes are more efficient according to the Second-Law of Thermodynamics, and their total exergy cost is lower.

Regarding the indicators employed, the unit exergy cost allows to compare schemes presenting the same or different production capacities, however, it does not allow to include the unit exergy cost of each product to calculate a total unit exergy cost of the products. On the other hand, the exergy cost of each product can be considered for the assessment of the total exergy cost; however, for comparing plants, they must have the same production capacities. For example, in the case Cogen 1 (CSP-MED 1), the unit exergy costs (of both products) are lower than in the Cogen 2 (CSP-MED 2), but the total energy cost is higher. This difference of both indicators is explained by the different capacities of the MED plant; therefore, the total exergy cost is not adequate to compare plants with different production capacities. Similarly, when comparing Cogen 7 (CSP-PH 3) and Cogen 8 (CSP-PH 4) schemes, the unit exergy cost of electricity is higher for the Cogen 7 (CSP-PH 3), but the unit exergy cost of heat is lower. Therefore, it is not possible to discriminate which configuration is better but considering that both plants have the same production capacities, then the total exergy cost can be used to compare them in detail. Therefore, Cogen 8 (CSP-PH 4) performs better than Cogen 7 (CSP-PH 3) because in the Cogen 8 (CSP-PH 4) scheme the total exergy cost is lower. In the case of the exergy efficiency, when comparing plants, the higher exergy efficiency does not necessarily imply that the plant is more convenient. For instance, in the Cogen 1 (CSP-MED 1) plant the exergy efficiency is lower than in the Cogen 2 (CSP-MED 2) plant, nevertheless, Cogen 1 (CSP-MED 1) is more convenient, as mentioned above.

3.2. *Comparison in multi-generation schemes*

According to Table 6, by comparing the cogeneration schemes, the most cost-effective options are Cogen 1 (CSP-MED 1), Cogen 3 (CSP-REF 1), and Cogen 6 (CSP-PH 2) to produce electricity-water, electricity-cooling, and electricity-process heat, respectively. These configurations presented the lower unit exergy cost of each product that were reached when MED plant replaced the condenser of the power cycle, the REF plant and the PH plant were coupled to a turbine extraction, in the CSP-MED, CSP-REF, and CSP-PH, respectively. Cogen 6 (CSP-PH 2) is close to Cogen 5 (CSP-PH 1) in terms of electricity cost, but it present about 12% of difference respecting the process heat cost. In the case of solar trigeneration schemes, Trigen 1 (CSP-MED-REF 1), Trigen 3 (CSP-REF-PH 1), and Trigen 7 (CSP-MED-PH 3) are the best options of each group of configurations, in which the MED plant replaced the condenser of the power cycle, and the REF plant and the PH plant were coupled to a turbine extraction. These options coincide with the best configurations obtained in the cogeneration schemes. Concerning the solar polygeneration schemes, the most cost-effective option is Poly 3, which also matches the best options above in terms of the coupling points of MED, REF, and PH plants. However, the choice between Poly 3 and

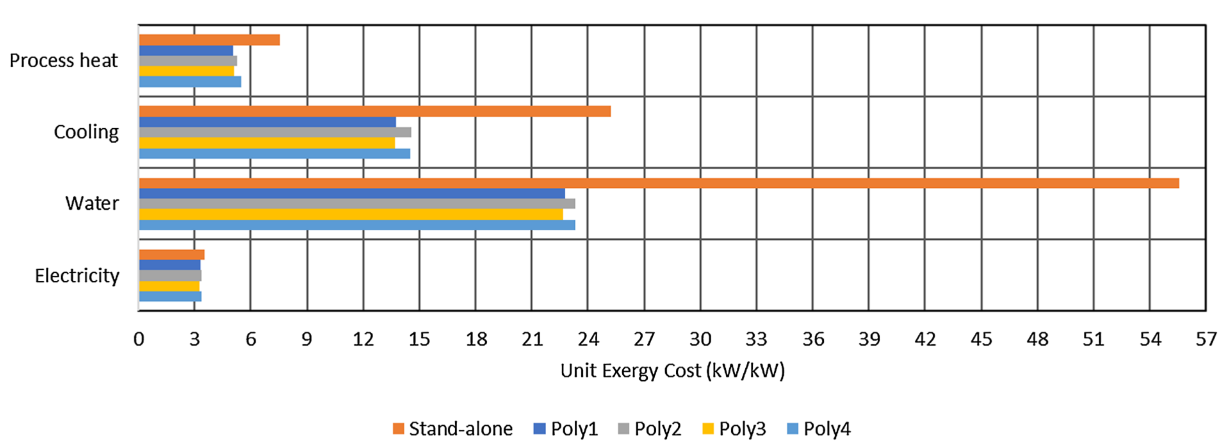

Fig. 7. Unit exergy cost of each product in stand-alone plants and polygeneration schemes.

Poly 1 is complex because the values of unit exergy cost of each product are very close, besides that, these options have different capacity of fresh water production. The total exergy cost is considered to discriminate which configuration is the best when the capacity of production is the same, as in Poly 2 and Poly 4. Then Poly 2 is more cost-effective than Poly 4, although the differences are quite close. Regarding the exergy costs distribution, the total exergy cost in Poly 3 is distributed as 75.3%, 20.7%, 1.8%, and 2.2% in electricity, water, cooling, and process heat, respectively. Finally, the most cost-effective options in multi-generation schemes (cogeneration, trigeneration, and polygeneration) are those in which the MED plant replaced the condenser of the power cycle, and the REF plant and the PH plant were coupled to a turbine extraction.

The main issues associated to the integration of MED, REF, and PH plants with a CSP plant, in cogeneration, trigeneration, or polygeneration schemes, are their technical restrictions, such as operating temperature constraints, size of the plants, coupling points in the CSP plant, and the flexibility to adjust the production to the demand of each product. The CSP plant generates electric power and rejects heat to the environment. The heat rejected from the power cycle could be used to produce the other products (fresh water, cooling, and process heat), whose production and sizing of plants are limited by the availability of the heat rejected. This type of configuration is named topping cycles [11] in which the supplied fuel is first used to produce power and then thermal energy, but not the other way around, and their priority is the power production. In this context, the main issues associated to the integration of MED plant is the flexibility to fix the water production independently of the electricity generation and that, in turn, depends on the MED coupling point. In a scheme where the MED plant operates as a base load water station, all configurations allow satisfying the demand, but only when the MED plant is coupled in a turbine extraction allows adjusting the water production to variable demand without

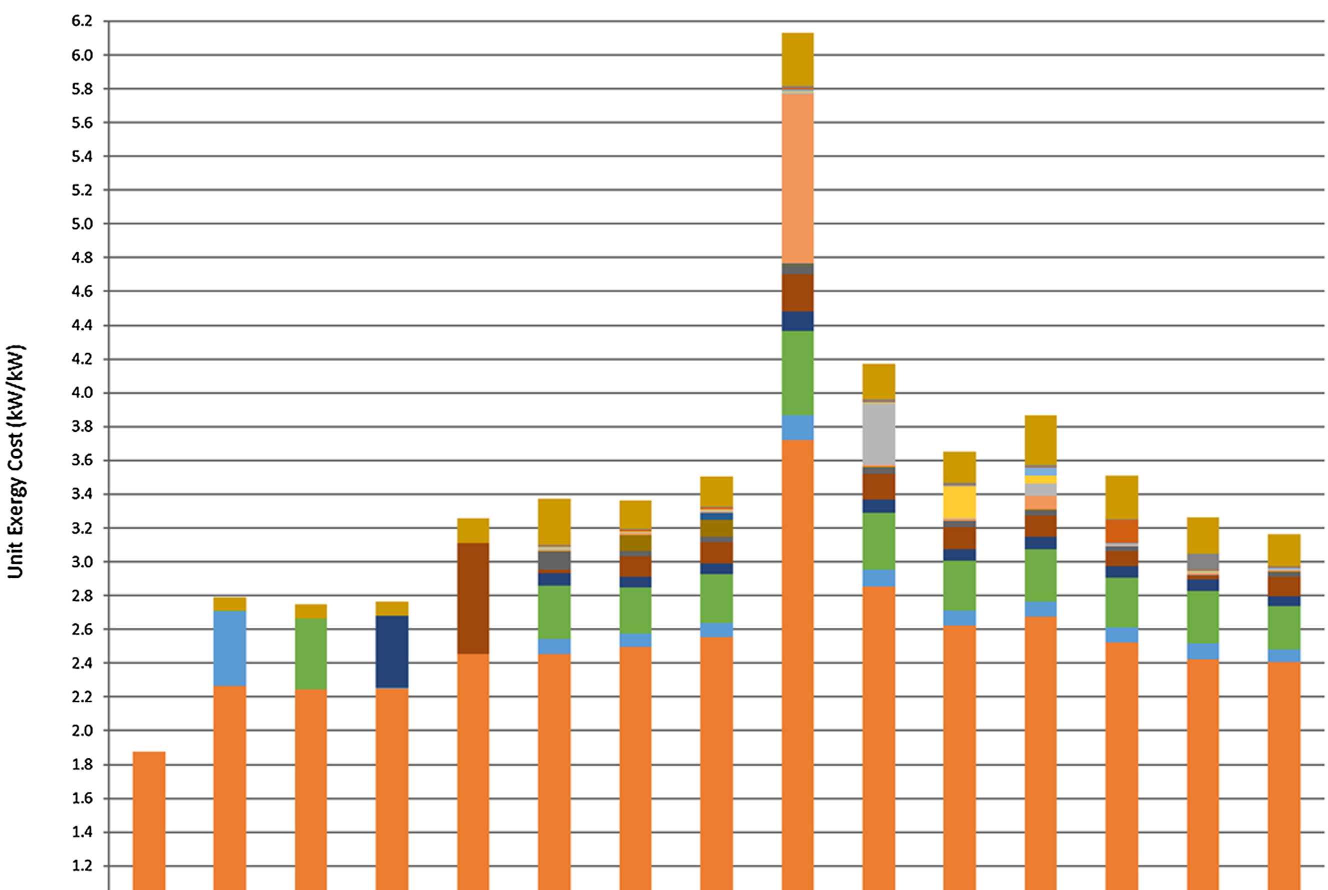

	Collectors	Economizer	Evaporator	Superheater	Reheater	HP_Turbine	LP_Turbine	Generator	FWP5	FWP4	FWP3	Deaerator	FWP2	FWP1	Condenser
Condenser	0.0000	0.0815	0.0802	0.0806	0.1446	0.2722	0.1716	0.1786	0.3125	0.2127	0.1862	0.2956	0.2578	0.2171	0.1884
FWP1	0.0000	0.0000	0.0000	0.0000	0.0000	0.0073	0.0064	0.0066	0.0116	0.0079	0.0069	0.0072	0.0069	0.0897	0.0060
FWP2	0.0000	0.0000	0.0000	0.0000	0.0000	0.0065	0.0056	0.0059	0.0103	0.0070	0.0061	0.0064	0.1342	0.0064	0.0053
Deaerator	0.0000	0.0000	0.0000	0.0000	0.0000	0.0049	0.0042	0.0044	0.0077	0.0052	0.0046	0.0459	0.0046	0.0048	0.0040
FWP3	0.0000	0.0000	0.0000	0.0000	0.0000	0.0053	0.0046	0.0048	0.0084	0.0057	0.1906	0.0502	0.0050	0.0052	0.0044
FWP4	0.0000	0.0000	0.0000	0.0000	0.0000	0.0076	0.0066	0.0069	0.0120	0.3623	0.0072	0.0715	0.0071	0.0074	0.0062
FWP5	0.0000	0.0000	0.0000	0.0000	0.0000	0.0083	0.0072	0.0075	1.0025	0.0090	0.0079	0.0784	0.0078	0.0082	0.0068
Generator	0.0000	0.0002	0.0002	0.0002	0.0003	0.0012	0.0011	0.0423	0.0019	0.0013	0.0012	0.0017	0.0011	0.0012	0.0010
LP_Turbine	0.0000	0.0006	0.0006	0.0006	0.0007	0.0027	0.0947	0.0986	0.0045	0.0031	0.0027	0.0039	0.0027	0.0027	0.0023
HP_Turbine	0.0000	0.0002	0.0002	0.0002	0.0002	0.1077	0.0304	0.0317	0.0555	0.0378	0.0331	0.0322	0.0220	0.0048	0.0286
Reheater	0.0000	0.0007	0.0007	0.0007	0.6545	0.0193	0.1210	0.1259	0.2203	0.1500	0.1313	0.1280	0.0873	0.0190	0.1137
Superheater	0.0000	0.0004	0.0004	0.4254	0.0004	0.0723	0.0630	0.0656	0.1147	0.0781	0.0684	0.0714	0.0683	0.0710	0.0592
Evaporator	0.0000	0.0016	0.4187	0.0016	0.0019	0.3140	0.2734	0.2847	0.4980	0.3390	0.2968	0.3098	0.2963	0.3082	0.2571
Economizer	0.0000	0.4416	0.0005	0.0005	0.0006	0.0937	0.0816	0.0850	0.1486	0.1012	0.0886	0.0925	0.0884	0.0920	0.0767
Collectors	0.8740	1.2656	1.2445	1.2515	1.4523	1.4515	1.4936	1.5552	2.7204	1.8518	1.6213	1.6723	1.5219	1.4247	1.4045
Environment	1.0000	1.0000	1.0000	1.0000	1.0000	1.0000	1.0000	1.0000	1.0000	1.0000	1.0000	1.0000	1.0000	1.0000	1.0000

Fig. 8. Cost decomposition in stand-alone CSP plant.

affecting the electricity production. Note that a base load on a system is the minimum level of demand over a span of time. The most cost-effective configurations of MED plant are Cogen 1 (CSP-MED 1), Trigen 1 (CSP-MED-REF 1), Trigen 7 (CSP-MED-PH 3), and Poly 3, but they are not necessarily the best solutions for the multi-generation system, because if the MED plant fails, it will affect the complete system. Respecting the integration of REF plant, these are associated with the operating temperature constraints of the desorber. Clearly, the REF plant should not replace the power plant condenser, nor should it be coupled in a turbine extraction that increases the turbine back pressure, such as Cogen 4 (CSP-REF 2) because it might affect the efficiency of the power cycle. The most cost-effective configurations of REF plant are Cogen 3 (CSP-REF 1), Trigen 3 (CSP-REF-PH 1), and Poly 3. Respecting the PH plant, the main issues also depend on the coupling point, the best location is in a turbine extraction, such as Cogen 6 (CSP-PH 2), Trigen 3 (CSP-REF-PH 1), Trigen 7 (CSP-MED-PH 3), and Poly 3. On the other hand, when the PH plant is coupled in the solar field, these cases are not favorable because the process heat module operates at a temperature higher than the temperature required. Finally, a failure event or maintenance stop in the CSP plant would affect all the plants, however, a failure or stop of any of the other plants (MED, REF, and PH) would not affect the others, except in the specific case in which the MED plant replaces the condenser.

3.3. Cost decomposition in stand-alone systems and solar multi-generation schemes

The cost decomposition for the stand-alone CSP plant are depicted in Fig. 8, showing how the unit cost of product is formed as the sum of the irreversibility contributions of the components and the residues (according to Eq. (12)). The unit exergy cost of electricity is 3.51 kW/kW, in which the contribution from the productive devices is 3.33 kW/kW and the contribution from the condenser (dissipative device) is 0.18 kW/kW. Note that the contribution from the environment is 1 kW/kW, according to the proposition stating that the cost of external resources is equal to its exergy (Eq. (10)). The main components that contribute to the cost formation of electricity (see generator in Fig. 8), in descending order of importance, are: solar collectors (44.3%), evaporator (8.1%), condenser (5.1%), reheater (3.6%), low-pressure turbine (2.8%), economizer (2.4%), superheater (1.9%), and generator (1.2%). The most significant exergy destruction is observed in the solar collectors, attributable to the irreversibilities associated to the large temperature difference between the sun and the heat transfer fluid. Furthermore, it is observed that the exergy cost is allocated to the rest of components according to a topping cycle scheme. Note that in a conventional steam power plant, the boiler is the main source of irreversibility [5]. Respecting the condenser that is a dissipative component, it is allocated to all productive units. It interacts with other components and allows to close the thermodynamic power cycle. As its operating temperature is quite low (36 °C) [4], from the point of view of the Second Law of Thermodynamics, its contribution to exergy costs is not significant, being the steam generator (or solar collectors in this case) the main inefficient component [17,40]. It is also possible to analyze the cost decomposition of any other component, such as FWPs, collectors or others; however, in these cases, it is important to study the cost decomposition in which the final product is generated (generator in Fig. 8). Finally, according to the results, it is recommended improving the design of the solar collectors to reduce their exergy destructed (irreversibilities) in the stand-alone CSP plant. An improved design can be achieved by increasing the optical efficiency of the collectors and reducing heat losses from the receiver [41,42]. Note that in the solar collectors, the solar exergy is distributed among the exergy optical losses, exergy destruction from the sun to the receiver, exergy thermal losses, exergy destruction from receiver to fluid, and useful exergy output; in which the exergy destruction from the sun to the receiver is the most important reason for the high irreversibility of solar collectors, followed by the exergy optical losses [41].

Fig. 9 shows the cost decomposition in the other stand-alone plants (MED, REF, and PH). The unit exergy cost of each product is the sum of the irreversibility contributions of the productive and dissipative devices that preceded the product generated, then the production cost of a component equals the cost of the resources required to obtain such product, as well as the cost of the residues generated. Consequently, the cost of the residues allocated to each productive component may be considered as external resources used to compensate the cost formation of the residues (see MED, REF, and PH in Fig. 9). The main contribution

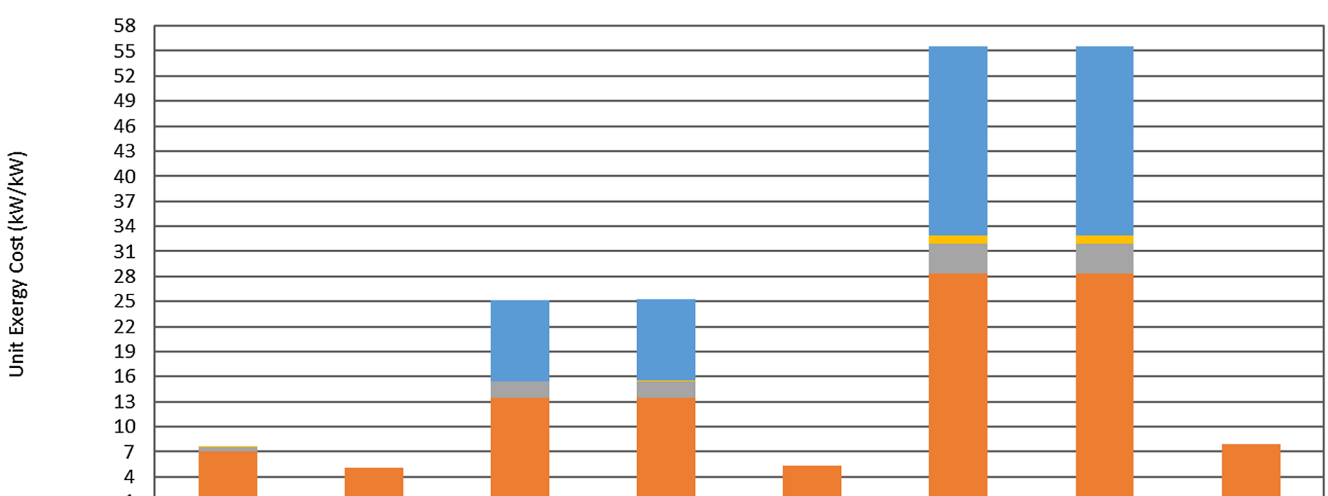

	PH	Boiler PH	Dissipator REF	REF	Boiler REF	Dissipator MED	MED	Boiler MED
Dissipator	0.000	0.000	9.722	9.738	0.000	22.693	22.693	0.000
Grid	0.002	0.000	0.046	0.046	0.000	0.926	0.926	0.000
Equipment	0.493	0.000	1.952	1.955	0.000	3.617	3.617	0.000
Boiler	6.064	4.065	12.467	12.486	4.271	27.310	27.310	6.873
Environment	1.000	1.000	1.000	1.000	1.000	1.000	1.000	1.000

Fig. 9. Cost decomposition in stand-alone MED, REF, and PH plants.

(a)

(b)

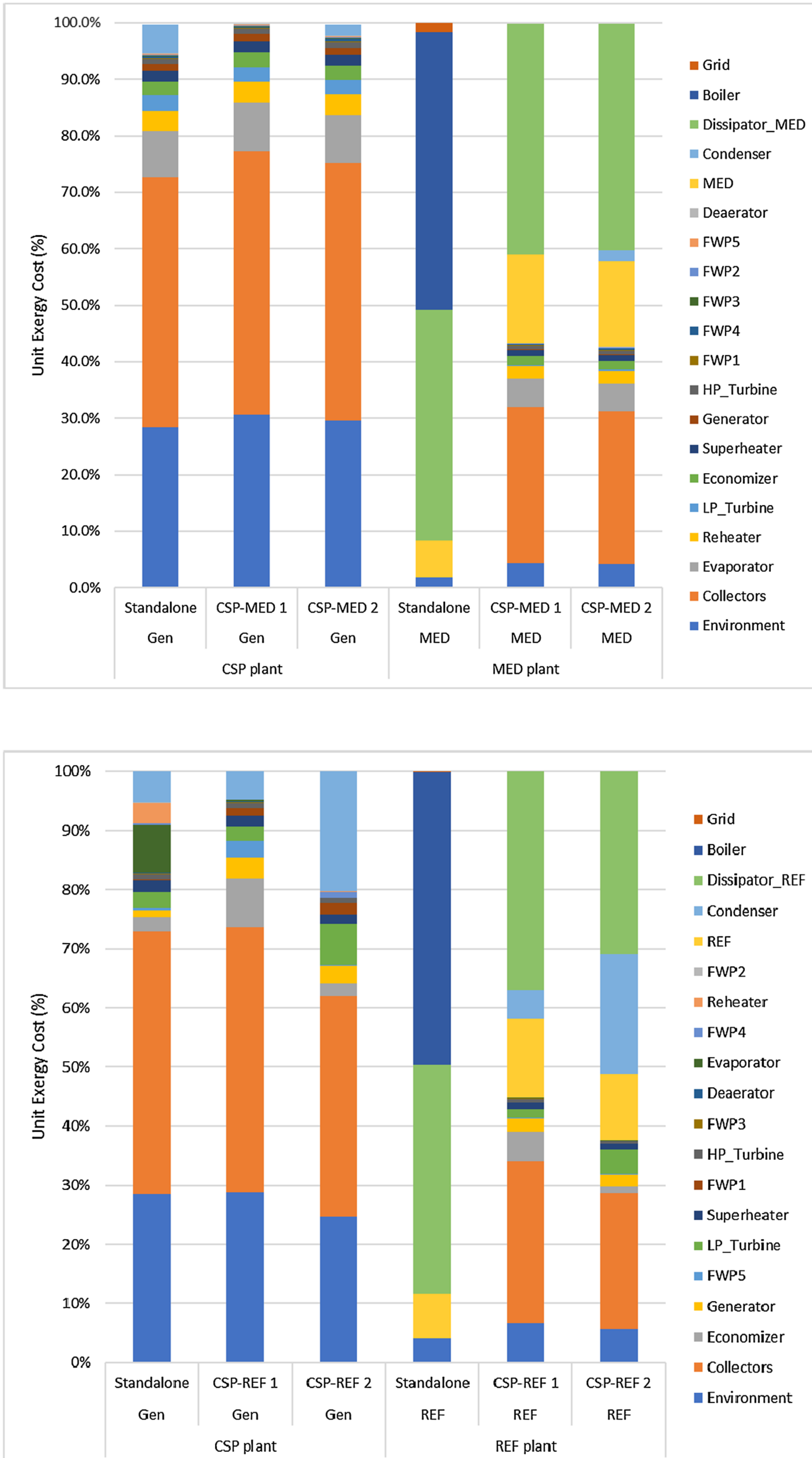

Fig. 10. Cost decomposition in cogeneration schemes. (a) CSP-MED. (b) CSP-REF. (c) CSP-PH.

in the cost of each product comes from the boiler with 49.2%, 49.5%, and 80.2% in MED, REF, and PH respectively, being the higher heat source and then having the higher exergy destruction. Note that, since both the MED plant and the REF plant include a dissipative component to operate, they participate in the cost formation with 40.9% and 38.6%, respectively. In the case of the PH, most of the exergy costs come from the boiler and a residual additional cost comes from the heat exchanger (6.5%) to accommodate the heat supply. Finally, considering the results, it is recommended improving the design in the boiler and the dissipative devices. In the first case, it could be improved the boiler

(c)

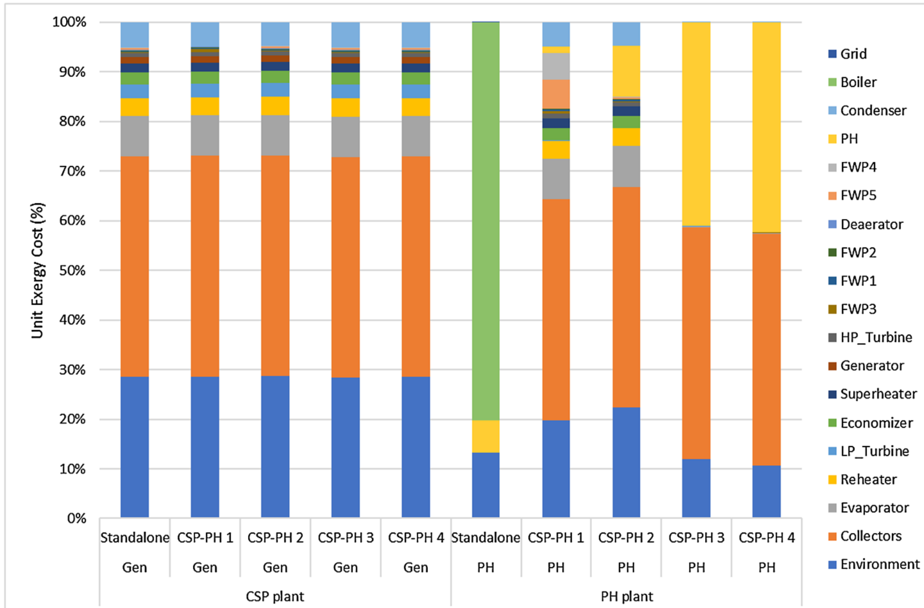

Fig. 10. (*continued*)

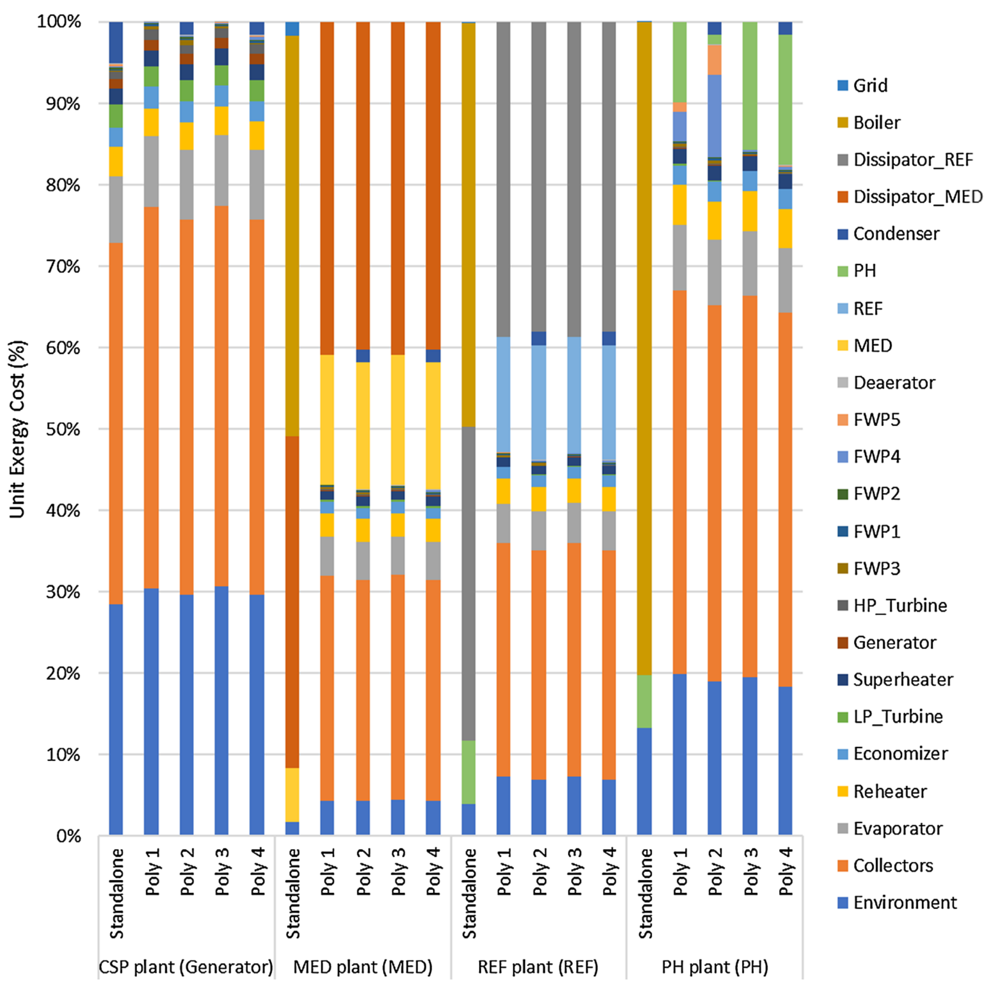

Fig. 11. Cost decomposition in polygeneration schemes.

design by reducing its exergy loss, such as preheating the air entering the boiler, reducing the temperature difference of the combustion products and steam, improving the insulation of boiler body, and controlling the amount of excess combustion air (fuel to air ratio) [43]. In the latter case, the design could be improved by optimizing the condensers or recovering the residual heat for use in other processes.

The method described above is based on the classification of the system flows in fuels, products, and residues, in which all costs yielded by the production process must be included in the cost of the final products. The residues are unintended remaining flows of matter or energy in any productive process. That flows could be partially used in further processes or become unusable or unwanted waste disposals [20]. Additionally, there are dissipative components, whose purpose is to eliminate the undesirable flows.

The cost decomposition in the cogeneration plants are depicted in Fig. 10 and Appendix A. Each scheme produces two products, electricity-water, electricity-cooling, and electricity-process heat (see Gen, MED, REF, and PH). Results show that the main contribution to the cost formation of the electricity are originated at the solar collectors, evaporator, reheater, and economizer. While regarding water, cooling, and process heat costs, the main contributions are: dissipative devices (MED and REF), solar collectors, productive subsystems (MED, REF, and PH), evaporator, reheater, economizer, and condenser (if the MED plant does not replace the condenser). In addition, the comparison between the stand-alone systems and each cogeneration scheme is shown in Fig. 10, in which the main difference is in the cost formation of the water, cooling, and process heat because these stand-alone plants are driven by the thermal energy from the boiler.

The detailed cost decomposition between the devices that generate each product in the trigeneration schemes analyzed is presented in Appendix B. The main components that contribute to the cost formation of electricity, water, and cooling, in the CSP-MED-REF schemes, are the solar collectors, evaporator, reheater, economizer, LP turbine, and superheater. Additionally, in the case of water and cooling, is included the MED's and REF's dissipative, MED, and REF. Concerning the CSP-REF-PH schemes, the main components that contribute to the cost formation of electricity, cooling, and process heat, are the solar collectors, evaporator, reheater, LP turbine, economizer, condenser, and superheater. In the case of water and cooling, additionally, it is included the REF's dissipative, REF, and PH. Lastly, in the CSP-MED-PH schemes, they are the solar collectors, evaporator, reheater, economizer, LP turbine, and superheater. Including the MED's dissipative, MED, and PH in the case of water and process heat. Respecting the comparison between the stand-alone systems and trigeneration schemes, the same tendencies of the cogeneration schemes are observed.

Finally, the cost decomposition in the polygeneration schemes analyzed are summarized in Fig. 11 and detailed in Appendix C. The main components that contribute to the cost formation of electricity in a solar polygeneration plant, in descending order of importance (considering the best configuration of polygeneration scheme as reference), are: solar collectors (46.6%), evaporator (8.7%), and reheater (3.4%). On the other hand, for the other products generated, the main components are dissipative device systems (40.9% in MED and 38.6% in REF), solar collectors (46.6% to 27.6%), productive subsystems (16.0% in MED, 14.3% in REF, and 15.6% in PH plants), evaporator (8.0% to 4.8%), and reheater (4.9% to 2.8%). Note that the same key components found are observed in all solar multi-generation schemes (cogeneration, trigeneration, and polygeneration) and in the stand-alone CSP plant. Nevertheless, in the other stand-alone plants (MED, REF, and PH) that are coupled to a boiler, the main contribution to the cost of water, cooling, and process heat is produced by the boiler itself. To reduce the costs of products, it is necessary to first consider these components in an in-depth process of analysis and optimization. Therefore, these components constitute the key equipment where the design should be improved. Regarding the cost of dissipative devices, there are still residues that cannot be reused in the integration processes analyzed. Hence, it is recommended searching for new integrations in order to reduce the effect of these residues, such as recovering the heat in the dissipative devices to be used in other processes.

In summary, in the solar multi-generation schemes, the solar collectors (solar field) represent the main contribution on cost formation of electricity and process heat, and it is the second for the water and cooling; while the MED's dissipative and REF's dissipative are the main components in cost formation of water and cooling, respectively. Those devices constitute the key components through which the design can be improved to reduce the cost of products. In the case of stand-alone systems, the key components are the same as in solar multi-generation schemes, except in the case of the stand-alone (MED, REF, and PH) plants in which the main contribution in the cost of water, cooling, and process heat comes from the boiler. Finally, the information provided by this analysis could show interesting relations that are not easy to discover using other methodologies.

4. Conclusions

Solar multi-generation schemes (cogeneration, trigeneration, and polygeneration) are an interesting option to generate power, fresh water, cooling, and process heat. Accordingly, the exergy cost theory (ECT) was applied to different solar multi-generation schemes (cogeneration, trigeneration, and polygeneration), and stand-alone systems to analyze the process of exergy cost formation, compare them, determine the key components to improve the design, detect potential energy savings, and establish the best configuration among these complex integrated schemes. The solar multi-generation schemes considered a concentrated solar power as the prime mover, a multi-effect distillation plant, a refrigeration plant, and a process heat unit. Twenty-one configurations were investigated, twenty of them regarding solar multi-generation plants: eight of cogeneration, eight of trigeneration, four polygeneration schemes, and the other considering stand-alone systems.

Symbolic Thermoeconomics is a branch of the ECT that provides a set of numerical procedures and general formulation, which is valid for any state of the system that depends only on the productive structure and its interaction with the environment. Also, it allows decomposing the production costs into the contributions of the components irreversibilities and residues cost, thus it describes the cost formation process in that solar multi-generation scheme. This method delivers information that is crucial for the design and optimization process of those complex schemes, since it allows identifying the key components that present the higher contribution to the unit exergy cost of product and reveals potential energy savings. Through a deep and detailed analysis of these components and their optimization, it is possible to reduce the costs of the final products.

The recommended configurations for the integrated solar multi-generation plants (cogeneration, trigeneration, and polygeneration) are those in which the MED plant replaces the condenser of the power cycle, and the refrigeration plant, as well as the process heat plant are coupled to turbine extractions. Those plants are the most cost-effective configuration because they deliver lower unit exergy costs of electricity, water, cooling, and heat.

The key equipment, on which the design should be improved in solar multi-generation schemes are: solar collector, productive subsystems (MED, refrigeration, and process heat plants), evaporator, and reheater because they are the main components that contribute to the costs formation of electricity, water, cooling, and process heat. For instance, those that contribute to the cost formation of electricity in Poly 3 are: solar collectors (46.6%) and evaporator (8.7%). For the other products are: dissipative device systems (40.9% in MED and 38.6% in REF), solar collectors (46.6% to 27.6%), and productive subsystems (16.0% in MED, 14.3% in REF, and 15.6% in PH plants).

It is recommended searching new integration schemes between the solar multi-generation systems to reduce the effect of the residues that cannot be reused internally yet, despite the integration. The new integrations schemes could consider the heat recovering in the dissipative devices to be used for other processes. For example, in the case of Poly 3, the dissipatives MED and REF contributes in 40.9% and 38.6% to the unit exergy cost of water and cooling, respectively. It must be considered that not all residues can be avoided, and the potential exergy saving is limited by technical and economic constraints.

The unit exergy cost, the total exergy cost, and the exergy efficiency are used to compare different configurations of multi-generation schemes. The unit exergy cost allows comparing any configuration, but in the case of the total exergy cost, it is used to compare only when the plants have the same production capacities. And in turn, a higher exergy efficiency does not imply that the plant is more convenient in thermoeconomic terms because, in general, the minimum total exergy cost and the maximum exergy efficiency are not reached for the same design point.

Solar multi-generation schemes, which include cogeneration, trigeneration, and polygeneration systems, are a promising alternative for the supply of electricity, fresh-water, cooling, and process heat for a zone with high irradiation conditions and scarcity of water, in which the CSP technology is the prime mover. Besides that, they are more cost-effective than stand-alone systems since these produce the lower unit exergy cost of each product. According to the results, the best option of polygeneration scheme allowed reducing the unit exergy cost on 6.8%, 59.2%, 45.6%, and 32.2%, for electricity, water, cooling, and process heat, respectively.

Acknowledgments

The authors wish to express their gratitude to CONICYT-PCHA/Doctorado_Nacional/año2013-folio21130634, and also appreciate the support from CONICYT/FONDAP 15110019 "Solar Energy Research Center" SERC-Chile, and the project Fondecyt N° 1130621.

Appendix A. Cost decomposition in the cogeneration plants

See Tables A1–A3.

Table A1
Cost decomposition of Generator and MED in CSP-MED plants (Cogen 1 and Cogen 2).

	Generator		MED	
Device/Cogen	1	2	1	2
Environment	30.7%	29.5%	4.3%	4.2%
Collectors	46.6%	45.7%	27.6%	27.0%
Evaporator	8.6%	8.4%	5.1%	5.0%
Reheater	3.7%	3.7%	2.2%	2.2%
LP_Turbine	2.6%	2.6%	0.3%	0.3%
Economizer	2.6%	2.5%	1.5%	1.5%
Superheater	2.0%	1.9%	1.2%	1.1%
Generator	1.3%	1.3%	0.1%	0.1%
HP_Turbine	1.0%	0.9%	0.6%	0.6%
FWP1	0.2%	0.2%	0.1%	0.1%
FWP4	0.2%	0.4%	0.1%	0.3%
FWP3	0.1%	0.1%	0.1%	0.1%
FWP2	0.1%	0.2%	0.1%	0.1%
FWP5	0.1%	0.1%	0.0%	0.1%
Deaerator	0.0%	0.1%	0.0%	0.1%
MED	0.0%	0.0%	15.7%	15.2%
Condenser	–	2.0%	–	2.0%
Dissipator_MED	0.0%	0.0%	40.9%	40.1%

Table A2
Cost decomposition of Generator and REF in CSP-REF plants (Cogen 3 and Cogen 4).

	Generator		REF	
Device/Cogen	3	4	3	4
Environment	28.6%	24.5%	6.6%	5.7%
Collectors	44.4%	37.3%	27.2%	22.9%
Economizer	8.1%	2.0%	5.0%	1.3%
Generator	3.6%	3.0%	2.2%	1.8%
FWP5	2.8%	0.1%	0.1%	0.1%
LP_Turbine	2.4%	6.8%	1.5%	4.2%
Superheater	1.9%	1.6%	1.1%	1.0%
FWP1	1.2%	2.0%	0.0%	0.0%
HP_Turbine	0.9%	0.8%	0.6%	0.5%
FWP3	0.2%	0.0%	0.1%	0.0%
Deaerator	0.2%	0.0%	0.1%	0.0%
Evaporator	0.1%	0.1%	0.1%	0.0%
FWP4	0.0%	1.0%	0.0%	0.0%
Reheater	0.0%	0.0%	0.0%	0.0%
FWP2	0.0%	0.1%	0.0%	0.0%
REF	0.0%	0.0%	13.3%	11.2%
Condenser	4.8%	20.1%	4.8%	20.1%
Dissipator_REF	0.0%	0.0%	36.8%	30.9%

Table A3
Cost decomposition of Generator and PH in CSP-PH plants (Cogen 5 to Cogen 8).

	Generator				PH			
Device/Cogen	5	6	7	8	5	6	7	8
Environment	28.5%	28.6%	28.4%	28.5%	19.6%	22.3%	12.0%	10.7%
Collectors	44.4%	44.4%	44.3%	44.3%	44.4%	44.4%	46.6%	46.6%
Evaporator	8.1%	8.1%	8.1%	8.1%	8.1%	8.1%	0.1%	0.1%
Reheater	3.6%	3.6%	3.7%	3.6%	3.6%	3.6%	0.1%	0.0%
LP_Turbine	2.8%	2.8%	2.8%	2.8%	0.2%	0.1%	0.0%	0.0%
Economizer	2.4%	2.4%	2.4%	2.4%	2.4%	2.4%	0.0%	0.0%
Superheater	1.9%	1.9%	1.9%	1.8%	1.9%	1.9%	0.0%	0.0%
Generator	1.2%	1.2%	1.2%	1.2%	0.1%	0.0%	0.0%	0.0%
HP_Turbine	0.9%	0.9%	0.9%	0.9%	0.9%	0.9%	0.0%	0.0%
FWP3	0.5%	0.2%	0.1%	0.1%	0.5%	0.2%	0.0%	0.0%
FWP1	0.2%	0.2%	0.2%	0.2%	0.2%	0.2%	0.0%	0.0%
FWP2	0.2%	0.2%	0.2%	0.2%	0.2%	0.2%	0.0%	0.0%
Deaerator	0.1%	0.1%	0.1%	0.1%	0.1%	0.1%	0.0%	0.0%
FWP5	0.1%	0.2%	0.2%	0.2%	5.8%	0.2%	0.0%	0.0%
FWP4	0.1%	0.2%	0.2%	0.2%	5.3%	0.2%	0.0%	0.0%
PH	0.0%	0.0%	0.0%	0.0%	1.4%	10.2%	40.8%	42.3%
Condenser	4.8%	4.8%	5.1%	5.1%	4.8%	4.8%	0.1%	0.1%

Appendix B. Cost decomposition in the trigeneration plants

See Tables B1–B3.

Table B1
Cost decomposition of Generator, MED, and REF in CSP-MED-REF plants (Trigen 1 and Trigen 2).

	Generator		MED		REF	
Device/Trigen	1	2	1	2	1	2
Environment	30.5%	29.5%	4.4%	4.3%	7.3%	6.9%
Collectors	46.6%	45.8%	27.6%	27.1%	28.6%	28.1%
Evaporator	8.7%	8.5%	4.8%	4.7%	4.9%	4.8%
Reheater	3.4%	3.4%	2.8%	2.7%	3.0%	3.0%
Economizer	2.6%	2.5%	1.4%	1.4%	1.5%	1.4%
LP_Turbine	2.5%	2.6%	0.3%	0.3%	0.1%	0.0%
Superheater	2.0%	2.0%	1.1%	1.1%	1.1%	1.1%
Generator	1.3%	1.3%	0.1%	0.1%	0.0%	0.0%
HP_Turbine	1.2%	1.1%	0.1%	0.1%	0.0%	0.0%
FWP1	0.2%	0.2%	0.1%	0.1%	0.1%	0.1%
FWP4	0.2%	0.4%	0.1%	0.2%	0.1%	0.2%
FWP3	0.2%	0.2%	0.1%	0.1%	0.1%	0.1%
FWP2	0.1%	0.2%	0.1%	0.1%	0.1%	0.1%
FWP5	0.1%	0.1%	0.0%	0.1%	0.0%	0.1%
Deaerator	0.0%	0.1%	0.0%	0.1%	0.0%	0.1%
MED	0.0%	0.0%	16.0%	15.5%	0.0%	0.0%
REF	0.0%	0.0%	0.0%	0.0%	14.3%	14.1%
Condenser	–	1.7%	–	1.7%	–	1.7%
Dissipator_MED	0.0%	0.0%	40.9%	40.2%	0.0%	0.0%
Dissipator_REF	0.0%	0.0%	0.0%	0.0%	38.6%	38.0%

Table B2
Cost decomposition of Generator, REF, and PH in CSP-REF-PH plants (Trigen 3 and Trigen 4).

	Generator		REF		PH	
Device/Trigen	3	4	3	4	3	4
Environment	28.7%	28.6%	6.7%	6.6%	17.4%	20.0%
Collectors	44.5%	44.5%	27.3%	27.3%	44.5%	44.5%
Evaporator	8.2%	8.2%	5.0%	5.0%	8.2%	8.2%
Reheater	3.6%	3.6%	2.2%	2.2%	3.6%	3.6%
LP_Turbine	2.7%	2.7%	0.1%	0.1%	0.1%	0.2%
Economizer	2.4%	2.4%	1.5%	1.5%	2.4%	2.4%
Superheater	1.9%	1.9%	1.2%	1.2%	1.9%	1.9%
Generator	1.2%	1.2%	0.0%	0.0%	0.0%	0.1%
HP_Turbine	0.9%	0.9%	0.6%	0.6%	0.9%	0.9%
FWP5	0.2%	0.1%	0.1%	0.0%	0.2%	6.2%
FWP1	0.2%	0.2%	0.1%	0.1%	0.2%	0.2%
FWP4	0.2%	0.1%	0.1%	0.0%	0.2%	5.1%
FWP2	0.2%	0.2%	0.1%	0.1%	0.2%	0.2%
FWP3	0.1%	0.5%	0.1%	0.3%	0.1%	0.5%
Deaerator	0.1%	0.1%	0.1%	0.1%	0.1%	0.1%
REF	0.0%	0.0%	13.3%	13.3%	0.0%	0.0%
PH	0.0%	0.0%	0.0%	0.0%	15.1%	0.9%
Condenser	4.5%	4.5%	4.5%	4.5%	4.5%	4.5%
Dissipator_REF	0.0%	0.0%	36.9%	36.9%	0.0%	0.0%

Table B3
Cost decomposition of Generator, MED and PH in CSP-MED-PH plants (Trigen 5 to Trigen 8).

	Generator				MED				PH			
Device/Trigen	5	6	7	8	5	6	7	8	5	6	7	8
Environment	30.4%	29.5%	30.5%	29.5%	4.4%	4.3%	4.4%	4.3%	19.9%	18.3%	19.5%	23.0%
Collectors	46.6%	45.8%	46.6%	45.8%	27.6%	27.1%	27.6%	27.1%	46.6%	45.8%	46.6%	45.8%
Evaporator	8.7%	8.5%	8.7%	8.5%	4.8%	4.7%	4.8%	4.7%	8.0%	7.9%	8.0%	7.8%
Reheater	3.4%	3.4%	3.4%	3.4%	2.8%	2.7%	2.8%	2.7%	4.9%	4.8%	4.9%	4.8%
Economizer	2.6%	2.5%	2.6%	2.5%	1.4%	1.4%	1.4%	1.4%	2.4%	2.3%	2.4%	2.3%
LP_Turbine	2.5%	2.6%	2.5%	2.6%	0.3%	0.3%	0.3%	0.3%	0.1%	0.1%	0.1%	0.1%
Superheater	2.0%	2.0%	2.0%	2.0%	1.1%	1.1%	1.1%	1.1%	1.8%	1.8%	1.8%	1.8%
Generator	1.3%	1.2%	1.3%	1.3%	0.1%	0.1%	0.1%	0.1%	0.1%	0.1%	0.0%	0.0%
HP_Turbine	1.2%	1.1%	1.2%	1.1%	0.1%	0.1%	0.1%	0.1%	0.1%	0.1%	0.0%	0.0%
FWP3	0.5%	0.5%	0.2%	0.2%	0.3%	0.3%	0.1%	0.1%	0.4%	0.5%	0.1%	0.2%
FWP1	0.2%	0.2%	0.2%	0.2%	0.1%	0.1%	0.1%	0.1%	0.2%	0.2%	0.2%	0.2%
FWP2	0.1%	0.2%	0.1%	0.2%	0.1%	0.1%	0.1%	0.1%	0.1%	0.2%	0.1%	0.2%
FWP4	0.1%	0.2%	0.1%	0.4%	0.0%	0.1%	0.1%	0.2%	3.1%	10.5%	0.1%	0.4%
FWP5	0.0%	0.1%	0.1%	0.1%	0.0%	0.0%	0.0%	0.1%	1.5%	3.2%	0.1%	0.1%
Deaerator	0.0%	0.1%	0.0%	0.1%	0.0%	0.1%	0.0%	0.1%	0.0%	0.1%	0.0%	0.1%
MED	0.0%	0.0%	0.0%	0.0%	15.9%	15.5%	16.0%	15.5%	0.0%	0.0%	0.0%	0.0%
PH	0.0%	0.0%	0.0%	0.0%	0.0%	0.0%	0.0%	0.0%	9.8%	1.8%	15.6%	11.1%
Condenser	–	1.8%	–	1.8%	–	1.8%	–	1.8%	–	1.8%	–	1.8%
Dissipator_MED	0.0%	0.0%	0.0%	0.0%	40.9%	40.1%	40.9%	40.1%	0.0%	0.0%	0.0%	0.0%

Appendix C. Cost decomposition in the polygeneration plants

See Tables C1 and C2.

Table C1
Cost decomposition of Generator and MED in CSP-MED-REF-PH plants (Poly 1 to Poly 4).

	Generator				MED			
Device/Poly	1	2	3	4	1	2	3	4
Environment	30.4%	29.6%	30.5%	29.6%	4.4%	4.3%	4.4%	4.3%
Collectors	46.6%	45.9%	46.6%	45.9%	27.6%	27.1%	27.6%	27.1%
Evaporator	8.7%	8.6%	8.7%	8.6%	4.8%	4.7%	4.8%	4.7%
Reheater	3.4%	3.4%	3.4%	3.4%	2.8%	2.7%	2.8%	2.7%
Economizer	2.6%	2.6%	2.6%	2.6%	1.4%	1.4%	1.4%	1.4%
LP_Turbine	2.5%	2.5%	2.5%	2.5%	0.3%	0.3%	0.3%	0.3%
Superheater	2.0%	2.0%	2.0%	2.0%	1.1%	1.1%	1.1%	1.1%
Generator	1.3%	1.3%	1.3%	1.3%	0.1%	0.1%	0.1%	0.1%
HP_Turbine	1.2%	1.2%	1.2%	1.2%	0.1%	0.1%	0.1%	0.1%
FWP3	0.5%	0.5%	0.2%	0.1%	0.2%	0.3%	0.1%	0.1%
FWP1	0.2%	0.2%	0.2%	0.2%	0.1%	0.1%	0.1%	0.1%
FWP2	0.1%	0.2%	0.1%	0.2%	0.1%	0.1%	0.1%	0.1%
FWP4	0.1%	0.1%	0.2%	0.4%	0.1%	0.1%	0.1%	0.2%
FWP5	0.0%	0.1%	0.1%	0.1%	0.0%	0.0%	0.0%	0.1%
Deaerator	0.0%	0.1%	0.0%	0.1%	0.0%	0.1%	0.0%	0.1%
MED	0.0%	0.0%	0.0%	0.0%	15.9%	15.5%	16.0%	15.5%
REF	0.0%	0.0%	0.0%	0.0%	0.0%	0.0%	0.0%	0.0%
PH	0.0%	0.0%	0.0%	0.0%	0.0%	0.0%	0.0%	0.0%
Condenser	–	1.5%	–	1.5%	–	1.6%	–	1.6%
Dissipator_MED	0.0%	0.0%	0.0%	0.0%	40.9%	40.2%	40.9%	40.2%
Dissipator_REF	0.0%	0.0%	0.0%	0.0%	0.0%	0.0%	0.0%	0.0%

Table C2
Cost decomposition of REF and PH in CSP-MED-REF-PH plants (Poly 1 to Poly 4).

	REF				PH			
Device/Poly	1	2	3	4	1	2	3	4
Environment	7.3%	6.9%	7.3%	6.9%	19.7%	18.9%	19.5%	18.3%
Collectors	28.6%	28.2%	28.6%	28.2%	46.6%	45.9%	46.6%	45.9%
Evaporator	4.9%	4.8%	4.9%	4.8%	8.0%	7.9%	8.0%	7.9%
Reheater	3.0%	3.0%	3.0%	3.0%	4.8%	4.8%	4.9%	4.8%
Economizer	1.5%	1.4%	1.5%	1.4%	2.4%	2.4%	2.4%	2.3%
LP_Turbine	0.1%	0.0%	0.1%	0.0%	0.2%	0.2%	0.1%	0.1%
Superheater	1.1%	1.1%	1.1%	1.1%	1.8%	1.8%	1.8%	1.8%
Generator	0.0%	0.0%	0.0%	0.0%	0.1%	0.1%	0.0%	0.0%
HP_Turbine	0.0%	0.0%	0.0%	0.0%	0.1%	0.1%	0.0%	0.0%
FWP3	0.3%	0.3%	0.1%	0.1%	0.4%	0.5%	0.1%	0.1%
FWP1	0.1%	0.1%	0.1%	0.1%	0.2%	0.2%	0.2%	0.2%
FWP2	0.1%	0.1%	0.1%	0.1%	0.1%	0.2%	0.1%	0.2%
FWP4	0.1%	0.1%	0.1%	0.2%	3.6%	10.0%	0.1%	0.4%
FWP5	0.0%	0.0%	0.0%	0.1%	1.2%	3.6%	0.1%	0.1%
Deaerator	0.0%	0.1%	0.0%	0.1%	0.0%	0.1%	0.0%	0.1%
MED	0.0%	0.0%	0.0%	0.0%	0.0%	0.0%	0.0%	0.0%
REF	14.2%	14.1%	14.3%	14.1%	0.0%	0.0%	0.0%	0.0%
PH	0.0%	0.0%	0.0%	0.0%	9.7%	1.2%	15.6%	15.9%
Condenser	–	1.6%	–	1.6%	–	1.6%	–	1.6%
Dissipator_MED	0.0%	0.0%	0.0%	0.0%	0.0%	0.0%	0.0%	0.0%
Dissipator_REF	38.6%	38.0%	38.6%	38.0%	0.0%	0.0%	0.0%	0.0%

References

[1] Serra LM, Lozano MA, Ramos J, Ensinas AV, Nebra SA. Polygeneration and efficient use of natural resources. Energy 2009;34(5):575–86.

[2] Al Moussawi H, Fardoun F, Louahlia-Gualous H. Review of tri-generation technologies: design evaluation, optimization, decision-making, and selection approach. Energy Convers Manage 2016;120:157–96.

[3] Modi A, Bühler F, Andreasen JG, Haglind F. A review of solar energy based heat and power generation systems. Renew Sustain Energy Rev 2017;67:1047–64.

[4] Leiva-Illanes R, Escobar R, Cardemil JM, Alarcón-Padilla D. Thermoeconomic assessment of a solar polygeneration plant for electricity, water, cooling and heating in high direct normal irradiation conditions. Energy Convers Manage 2017;151(May):538–52.

[5] Leiva-Illanes R, Escobar R, Cardemil JM, Alarcón-Padilla D. Comparison of the levelized cost and thermoeconomic methodologies – Cost allocation in a solar polygeneration plant to produce power, desalted water, cooling and process heat. Energy Convers Manage 2018;168(Jul.):215–29.

[6] Nuorkivi A. Allocation of fuel energy and emissions to heat and power in CHP. Energy-AN Consulting; 2010. Available: < http://era17.fi/wp-content/uploads/2012/02/Report-Nordic-CHP-Allocation_Energy-AN-Consulting_2010-9-7.pdf > . [Accessed: 24-Aug-2017].

[7] Bejan A, Tsatsaronis G, Moran M. Thermal design and optimization. 1st ed. John Wiley & Sons; 1996.
[8] Abusoglu A, Kanoglu M. Exergoeconomic analysis and optimization of combined heat and power production: a review. Renew Sustain Energy Rev Dec. 2009;13(9):2295–308.
[9] Valero A, Usón S, Torres C, Valero A, Agudelo A, Costa J. Thermoeconomic tools for the analysis of eco-industrial parks. Energy 2013;62:62–72.
[10] Valero A, Lerch F, Serra L, Royo J. Structural theory and thermoeconomic diagnosis. Energy Convers Manage 2002;43(9–12):1519–35.
[11] Jana K, Ray A, Majoumerd MM, Assadi M, De S. Polygeneration as a future sustainable energy solution – A comprehensive review. Appl Energy 2017;202:88–111.
[12] NREL. Aalborg CSP-Brønderslev CSP with ORC project. SolarPACES; 2017. Available: < https://www.nrel.gov/csp/solarpaces/project_detail.cfm/projectID=8316 > . [Accessed: 06-Jul-2017].
[13] Al-Sulaiman FA, Dincer I, Hamdullahpur F. Thermoeconomic optimization of three trigeneration systems using organic Rankine cycles: Part I – Formulations. Energy Convers Manage 2013;69(May):199–208.
[14] Al-Sulaiman FA, Dincer I, Hamdullahpur F. Thermoeconomic optimization of three trigeneration systems using organic Rankine cycles: Part II – Applications. Energy Convers Manage 2013;69(May):209–16.
[15] Calise F, d'Accadia MD, Macaluso A, Piacentino A, Vanoli L. Exergetic and exergoeconomic analysis of a novel hybrid solar–geothermal polygeneration system producing energy and water. Energy Convers Manage 2016;115:200–20.
[16] Ortega-Delgado B, García-Rodríguez L, Alarcón-Padilla D. Thermoeconomic comparison of integrating seawater desalination processes in a concentrating solar power plant of 5 MWe. Desalination 2016;392:102–17.
[17] Mehrpooya M, Ghorbani B, Sina S. Thermodynamic and economic evaluation of a novel concentrated solar power system integrated with absorption refrigeration and desalination cycles. Energy Convers Manage 2018;175(August):337–56.
[18] Wellmann J, Meyer-Kahlen B, Morosuk T. Exergoeconomic evaluation of a CSP plant in combination with a desalination unit. Renew. Energy 2018;128:586–602.
[19] Leiva-Illanes R, Escobar R, Cardemil JM, Alarcón-Padilla D, Uche J, Martínez A. Exergy cost decomposition and comparison of integrating seawater desalination plant, refrigeration plant, process heat plant in a concentrated solar power plant. In: Conference proceedings, ISES solar world congress, IEA SHC international conference on solar heating and cooling for buildings and industry; 2017. p. 125–35.
[20] Torres C, Valero A, Rangel V, Zaleta A. On the cost formation process of the residues. Energy 2008;33(2):144–52.
[21] Usón S, Valero A, Agudelo A. Thermoeconomics and industrial symbiosis. effect of by-product integration in cost assessment. Energy 2012;45(1):43–51.
[22] Torres C, Valero A, Serra L, Royo J. Structural theory and thermoeconomic diagnosis. Energy Convers Manage 2002;43(9–12):1503–18.
[23] NREL. System Advisor Model (SAM) Case Study: Andasol-1; 2013. p. 1–10.
[24] Wagner MJ, Gilman P. Technical manual for the SAM physical trough model. Contract 2011;303(June):275–3000.
[25] Blanco-Marigorta AM, Victoria Sanchez-Henríquez M, Peña-Quintana JA. Exergetic comparison of two different cooling technologies for the power cycle of a thermal power plant. Energy 2011;36(4):1966–72.
[26] Zak G, Mitsos A, Hardt D. Thermal desalination: structural optimization and integration in clean power and water Master Thesis Massachusetts Institute of Technology; 2012.
[27] Herold K, Radermacher R, Klein S. Absorption chillers and heat pumps. 1st ed. CRC Press; 1996.
[28] El-Dessouky H, Ettouney H. Fundamentals of salt water desalination. Elsevier; 2002.
[29] Al-Karaghouli A, Kazmerski LL. Energy consumption and water production cost of conventional and renewable-energy-powered desalination processes. Renew Sustain Energy Rev 2013;24:343–56.
[30] Sarbu I, Sebarchievici C. General review of solar-powered closed sorption refrigeration systems. Energy Convers Manage 2015;105(Nov.):403–22.
[31] Palenzuela P, Alarcón-Padilla D, Zaragoza G. Large-scale solar desalination by combination with CSP: techno-economic analysis of different options for the Mediterranean Sea and the Arabian Gulf. Desalination 2015;366:130–8.
[32] Escobar RA, Cortés C, Pino A, Pereira EB, Martins FR, Cardemil JM. Solar energy resource assessment in Chile: satellite estimation and ground station measurements. Renew Energy 2014;71(Nov.):324–32.
[33] SimTech GmbH. IPSEpro Process Simulation Environment. Rev 5.0. SimTech Simulation Technology; 2011.
[34] Torres C, Valero A. ExIO, Thermoeconomic analysis of thermal systems. CIRCE, Universidad de Zaragoza; 2012.
[35] Valero A, Torres C. Thermoeconomic analysis. Exergy, energy system analysis and optimization - encyclopedia of life support systems (EOLSS); 2016.
[36] Palacios-Bereche Reynaldo NS, Gonzales R. Exergy calculation of lithium bromide–water solution and its application in the exergetic evaluation of absorption refrigeration systems LiBr–H2O. Int J Energy Res 2012;36:166–81.
[37] Sharqawy MH, Lienhard V JH, Zubair SM. On exergy calculations of seawater with applications in desalination systems. Int J Therm Sci 2011;50(2):187–96.
[38] Ahmadi P, Dincer I, Rosen MA. Exergy, exergoeconomic and environmental analyses and evolutionary algorithm based multi-objective optimization of combined cycle power plants. Energy 2011;36(10):5886–98.
[39] Petela R. Engineering Thermodynamics of Thermal Radiation for solar Power Utilization. 1st ed. McGraw-Hill Education; 2010.
[40] Adibhatla S, Kaushik SC. Exergy and thermoeconomic analyses of 500 MWe sub critical thermal power plant with solar aided feed water heating. Appl Therm Eng 2017;123:340–52.
[41] Bellos E, Tzivanidis C. A detailed exergetic analysis of parabolic trough collectors. Energy Convers Manage 2017;149:275–92.
[42] Zare V, Moalemian A. Parabolic trough solar collectors integrated with a Kalina cycle for high temperature applications: energy, exergy and economic analyses. Energy Convers Manage 2017;151(August):681–92.
[43] Ahmadi GR, Toghraie D. Energy and exergy analysis of Montazeri Steam Power Plant in Iran. Renew Sustain Energy Rev 2016;56:454–63.